Fluid and Solid Fibers Made of Lipid Molecular Bilayers

Jürgen-Hinrich Fuhrhop*

Institut für Organische Chemie der Freien Universität Berlin, Takustrasse 3, D-1000 Berlin 33, Germany

Wolfgang Helfrich

Institut für Theoretische Physik der Freien Universität Berlin, Arnimallee 14, D-1000 Berlin 33, Germany

Received September 2, 1992 (Revised Manuscript Received January 25, 1993)

Contents

I. Introduction

Amphiphiles self-organize in water to form molecular bilayers.[1-7] The hydrophobic effect causes aggregation and holds the bilayer together. Repulsive hydration and steric forces, on the other hand, prevent the formation of large, three-dimensional crystals.[2] The most common appearances of such bilayers are infinite planar bilayers ("Myelin figures"), spherical or tubular vesicles, and micelles. In all cases the viscous hydrophobic center[5] of the aggregates is completely filled by hydrocarbon chains, whereas relative large distances prevail between the head groups (Figure 1, parts a and c). The head-group arrangements can therefore be considered to be fluidlike. This character is most pronounced in highly curved micellar aggregates irrespective of the model used (Figure 1a),[3-5] but is also present in planar bilayers (Figure 1c).[6,7] Actually the existence of bimolecular assemblies in aqueous suspensions is thought to depend on repulsive hydration and sterical forces between the head groups as well as on the binding hydrophobic forces.[2,7]

Within the last five years or so it became, however, apparent to us that bimolecular micellar rods and ribbons with lengths of several micrometers and a width of 4 nm[8,9] cannot have a fluid surface. Well-defined helical structures in rods and ribbons in which each molecule is in direct contact with water can certainly not be formed by nondirectional repulsive forces. Dissolution of a few molecules would destroy such fibers. Furthermore, such structures are formed by single-chain amphiphiles with as few as eight methylene groups so that the hydrophobic effect is relatively weak. One must therefore assume *overall binding forces between the head groups* in order to account for the stability of the micellar and vesicular fibers (Figure 1, parts b and d). Secondary amide hydrogen bond chains have been found to be the most useful and general stabilizing factor to overcome dissolving hydration energies. Several typical examples (C–H) of lipid aggregates with crystalline surfaces are given in Figure 2.

In this review we shall give a survey on elongated micellar and vesicle systems in both the fluid and solid state.

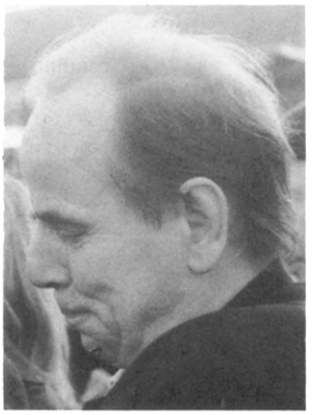

Jürgen-Hinrich Fuhrhop has been Professor of Organic Chemistry at the Freie Universität Berlin since 1978. His thesis in Braunschweig with Prof. H. H. Inhoffen and postdoctoral work at the Rockefeller University (New York) with Profs. D. Mauzerall and S. Granick was about the oxidation of metalloporphyrins to radicals and bile pigments. Currently, his research concerns the understanding and application of synthetic supramolecular lipid and porphyrin assemblies. (The above photograph was taken at the Berlin wall the morning after its opening, November 10th, 1989.)

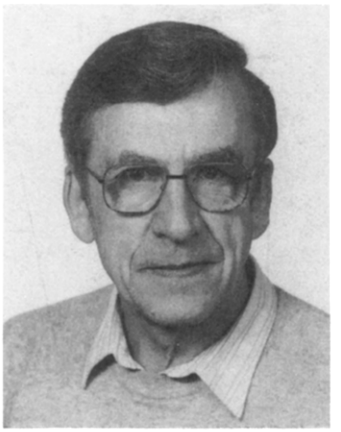

Wolfgang Helfrich has been Professor of Physics at the Freie Universität Berlin since 1973. His thesis was about space charge limited currents in anthracene crystals. He then moved on to liquid crystals, being one of the inventors of the twisted-nematic display. His present main area of research is biological model membranes. In 1976 he was awarded the Hewlett-Packard Europhysics Prize.

0009-2665/93/0793-1565$12.00/0

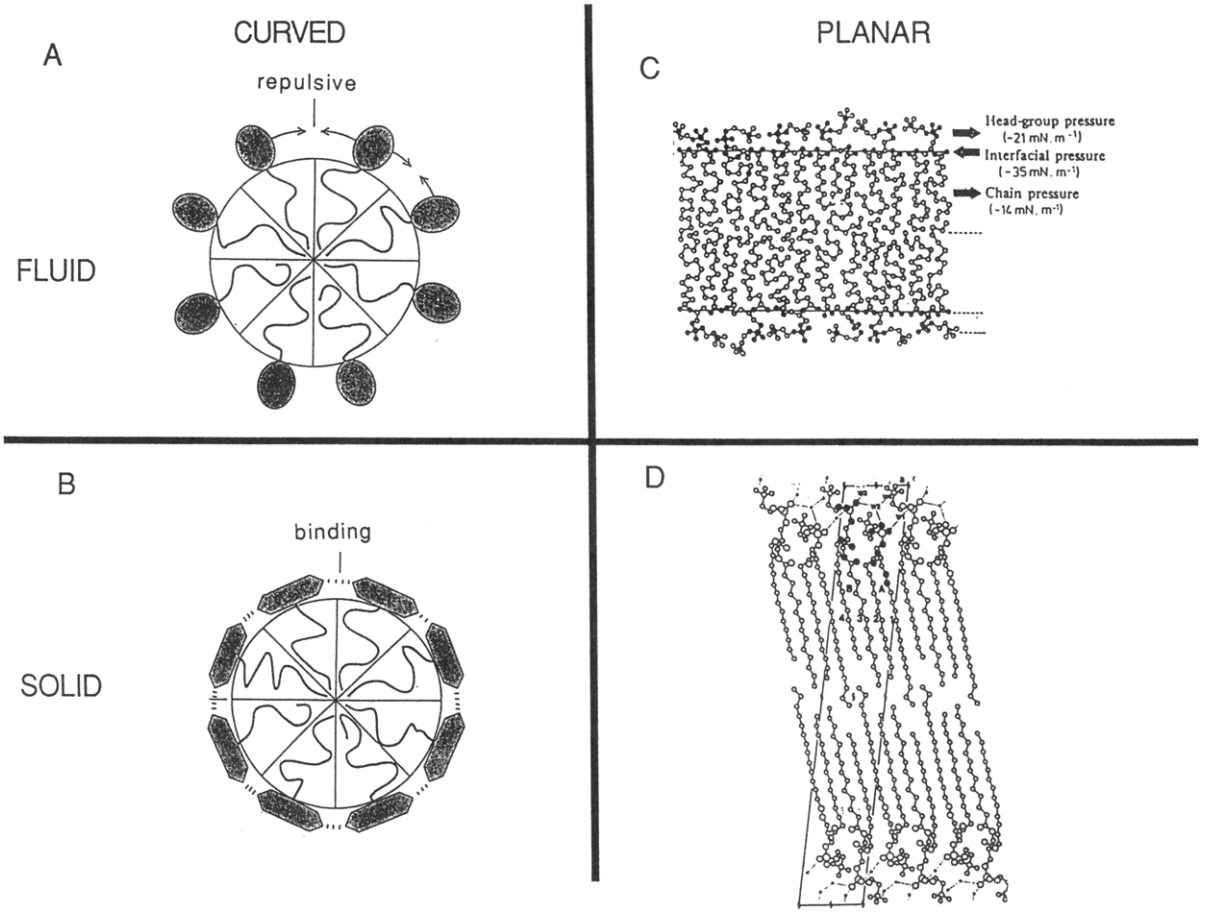

Figure 1. Schematic cross-sections through (A) a fluid micellar rod, (B) a solid micellar rod with a crystalline surface, (C) a fluid planar bilayer, and (D) a crystalline planar bilayer.[2,7]

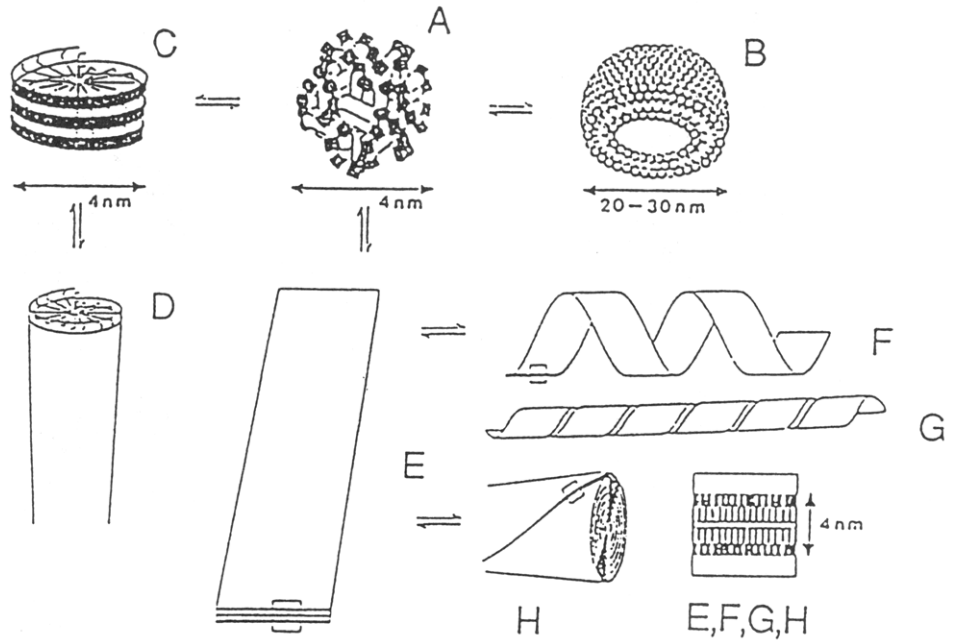

Figure 2. Spherical micelles (A) and vesicles (B) show, in general, repulsive interactions of the head groups. They have a fluid surface. If the head groups of micelles crystallize disk micelles (C) are probably formed first, which immediately aggregate to form bilayer rods (D). Micelles or vesicles may also form bilayer sheets (E) with strong binding interactions on the surface. They may bend to form helical ribbons (F) and mono- or multilayer tubules (G and H).

II. Rods

The best-known examples for fluid rod structures are formed by swelling of lecithin multilayer crystallites in water. They are of light-microscopic dimensions and belong to the Myelin figures. In the first step simple rods of 20–40-μm diameter ($\sim$250 molecular bilayers) grow into the medium and produce many irregular foldings without changing the width (Figure 3a). The second step is characterized by much slower growth

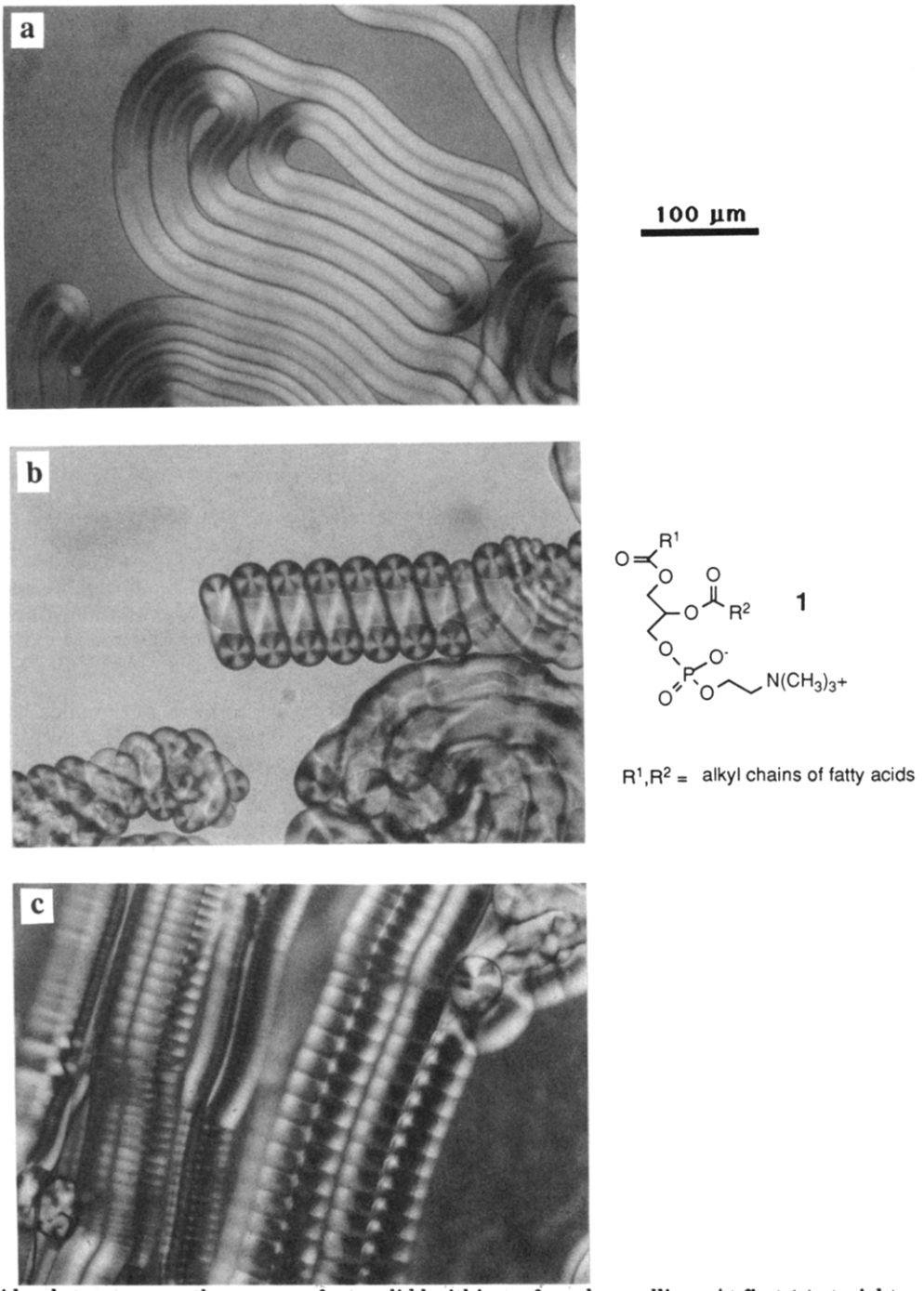

Figure 3. Fluid rod structures as they emerge from solid lecithin surfaces by swelling. At first (a) straight rods with irregular twistings are observed which later (b) may become helical and (c) grow to raillike structures. These structural changes are *not* reversed by dilution or by heating. Reprinted from ref 10. Copyright 1985 Gordon & Breach (London) (with kind permission of Prof. I. Sakurai).

rates and the appearance of several helical and coiling forms (Figure 3b). In the third and final step contacting helices and coils fuse into oily streaks (Figure 3c) and complex mosaic structures.[10] The fluid character of all these structures becomes apparent by the continuous changes of the structures upon flow of new material from the lecithin crystals to the 20–40-μm rods.

It has also been known for a long time that myelin figures[11,12] are reversibly transformed to microvesicles (diameter 20–30 nm) by ultrasonication. Precipitation usually takes a few days and proceeds via intermediate large vesicles. Spontaneous fusion and fission of vesicles have been traced to a change of elasticity module of the membrane.[13] This can be brought about by different environmental conditions (temperature, salt concentrations) or dissolution of rigid molecules in the bilayer membrane (e.g. cholesterol).

Multilayered rods offer no possibilities for supramolecular ordering. The position of dissolved or attached functional molecules can neither be fixed nor be determined with any certainty. Thinner surfactant rods are more promising. A very long-lived type of micellar rods with very high length to diameter ratios is obtained in 10^{-3}–10^{-2} M clear aqueous suspensions of cetyltrimethylammonium bromide **2** (Figure 4) in the presence of equimolar amounts of salicylic acid.[14,15] These rods have a diameter of about 12 nm, which corresponds to three molecular bilayers. Several holes in the fiber point

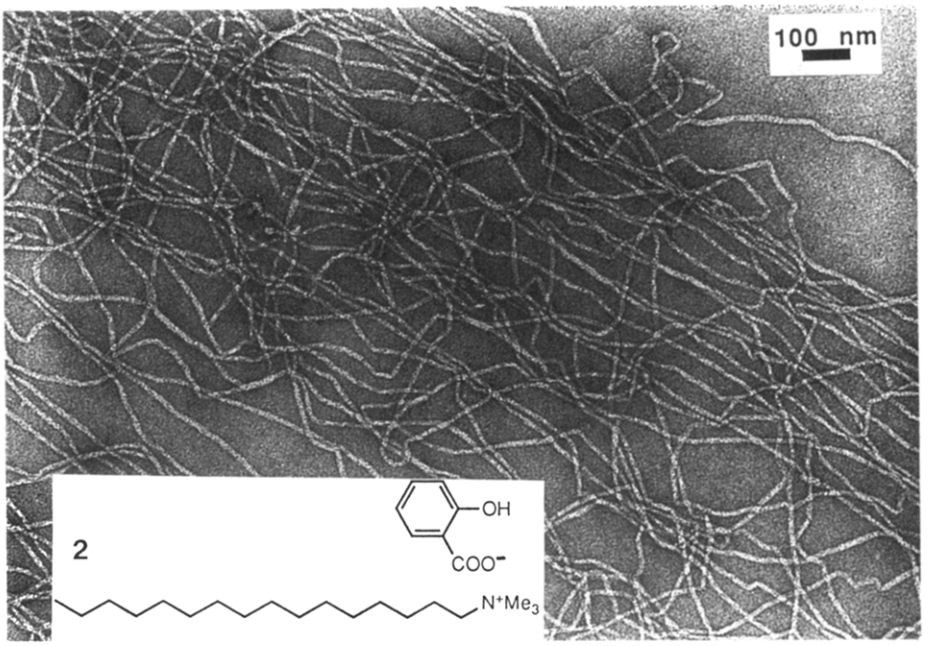

Figure 4. Cetyltrimethylammonium bromide (CTAB) with salicylic acid (SA) as counterion forms long fibers in water with a constant diameter of 12 nm. Reprinted from ref 14. Copyright 1987 Japanese Society of Electron Microscopy (with kind permission of Prof. H. Hirata).

to separations in bundles of single fibers. It might well be that this fiber is a quadruple rod (see below). The effect of the phenol (or phenolate?) on fiber formation has to the best of our knowledge not been explained in the literature. It is known, however, that salicylic acid, *o*- and *p*-iodophenol, and *p*-toluic acid have strong fiber-inducing effects in a 1:1 molar ratio and at concentrations between 10^{-3} and 10^{-2} M. Other hydroxybenzoic acids, diphenols, etc., have less or no effect. Fiber formation from micelles thus depends on the action of phenolic entrapments or counterions. It has also been shown by ^{1}H NMR spectroscopy that sodium salicylate is immobilized and binds to the ammonium head groups.[16] It seems likely that the polarizable phenol molecules form stacks and thus align the cetyltrimethylammonium chains. Talmon has characterized uniform rods of 5-nm diameter by cryoelectron microscopy.[17] This corresponds to a molecular bilayer. More work is needed to clarify the molecular structure of these fascinating molecular assemblies, which seem to be on the borderline between fluid and solid micellar rods. Their formation occurs by some type of precipitation which is typical for solid micellar fibers. The binding forces between the head group molecules (tetraalkylammonium and phenol) are, however, relatively weak. Therefore, the fibers are not as stiff and uniform as the fibers described below.

Helical 12-nm-thick rods have been obtained from 12-hydroxy stearic acid in organic solvents.[18a,b] These organogels will not be further discussed here, since organic fibers in organic solvents do not promise anything for the construction of supramolecular reaction systems. Only in aqueous environments does the clean separation of organic constituents of complex reaction systems seem possible. If the water-insoluble compound *N*-octyl-D-gluconamide (**3**) is heated in aqueous suspensions above 80 °C, spherical micelles are formed. They show a sharp transition point in scanning differential calorimetry at 78 °C. At this temperature amide hydrogen bond chains are formed in a cooperative process and helical rod structures appear immediately.[8,19] At pH 4 and in the presence of phosphotungstate ultrathin (diameter 3.8 nm) bulgy helices are trapped which are thought to be in equilibrium with micellar disks (Figure 2c).[9,20] The evidence for their disk character comes first from their tendency to form extremely long helical rods and second from their solution ^{1}H NMR spectrum, which shows frozen hydrocarbon chains and flexible carbohydrate head groups.[20] A detailed electron microscopic study of these helices revealed a quadruple helix with a magic-angle (54.7°) inclination (Figure 5), which is probably dictated by order electric interactions between the four helices.[21] The cooperative energy of interactions in the side–side contacts especially in the knots stabilizes the micellar fiber. A couple of geometrical rules, rather than molecular conformations, dominate the crystalline order of the fiber. The pitch corresponds, for example, to $2\pi \times$ bilayer thickness, the bulges' radius is $\sqrt{2} \times$ bilayer thickness, etc. As a whole, the quadruple helix lies on a minimal surface[21,22] and shows optimal electron microscopic definition and simplicity. Each single molecule is in contact with water and the fiber has a very sharp melting point of 79.6 °C.[8] At this temperature the amide hydrogen bonds dissociate in a cooperative process and the whole fiber disintegrates. These findings clearly indicate that binding forces between the head groups hold together the helical molecular bilayer. The micellar surface is therefore microcrystalline, not fluid. The individual fibers most often show statistical disorder, but they can be aligned on solid surfaces by mechanical means such as rapid drying by suction with filter paper.[21]

Introduction of negative charge into the gluconamide fiber plus binding of a planar aromatic system was achieved in the monophthalate (Figure 6). This compound gives very stable micellar fibers at pH = 5.[23] The exact multiplicity of strands in these fibers is not known, but a double or quadruple strand seems likely. Again no alignment is evident.

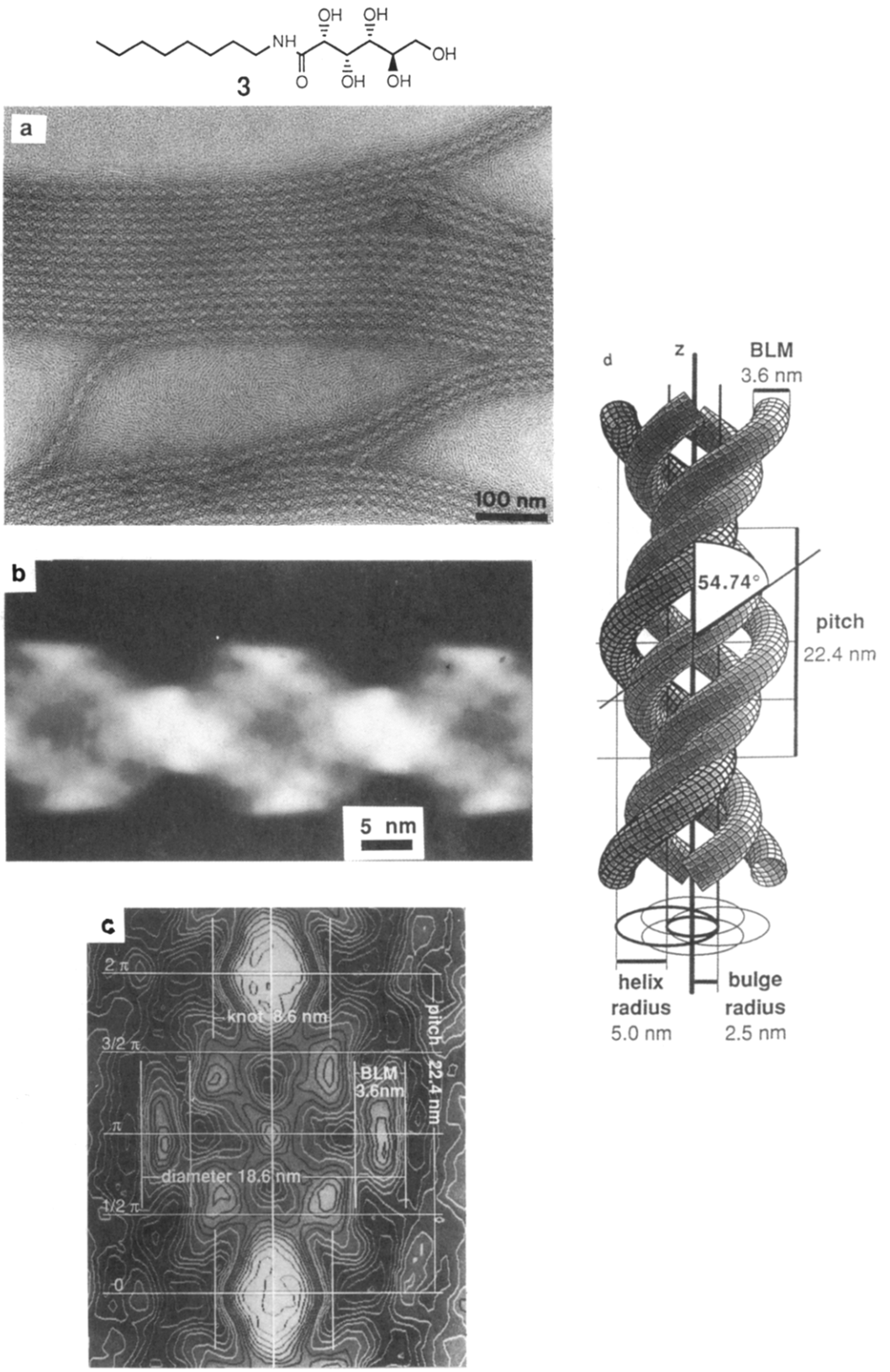

Figure 5. A well-defined molecular bilayer assembly in form of a quadruple helix has been obtained from *N*-octyl-D-gluconamide (**3**):[21] (a) electron micrograph of a fiber bundle; (b) magnification of a; the diameter of the white knots is 7.4 nm; (c) contour line diagram obtained by image analysis; (d) computer model of the fiber.

The closely related tartaric acid amide **5** dissolves in water at pH 8 and aggregates to aligned single micellar fibers at pH 5 (Figure 7). Depending on the counterion and concentration one finds either tubules (see section 5) or very large sheets in which the individual micellar strands remain visible under the electron microscope.[24] Such sheets have been called "bilayer cloths". They may assemble to multilayers and then reach sizes of several square millimeters. They are *not* to be confused with the continuous bilayer sheets or lamellae of myelin figures.

The multiplicity of lipid micellar rods in the observed structures is only known in the case of the quadruple helix (Figure 5). The micellar strands of the tartaric

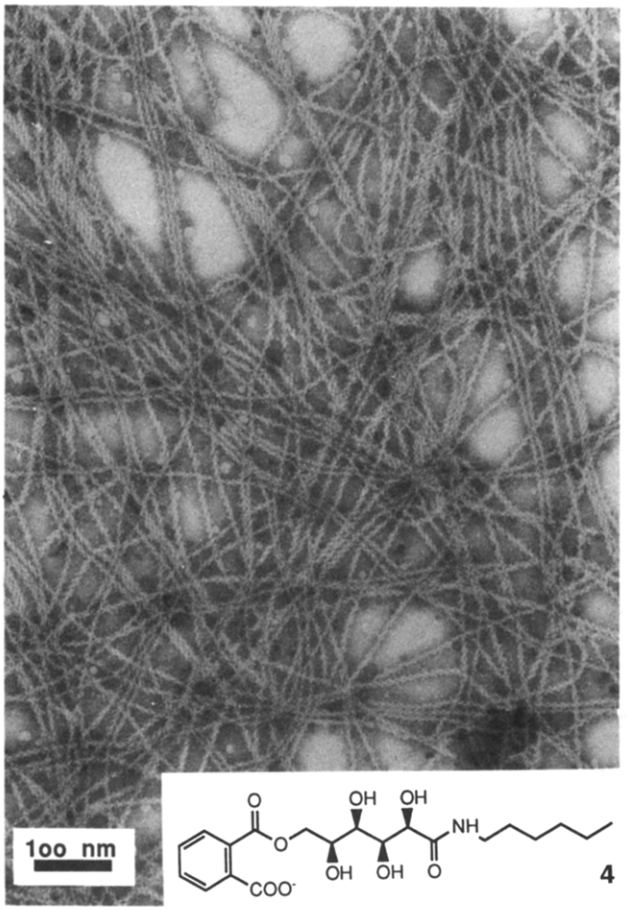

Figure 6. The micellar fibers made of the anionic gluconamide **4** (width 4–5 nm) can be packed very tightly. No merging occurs. Reference 23.

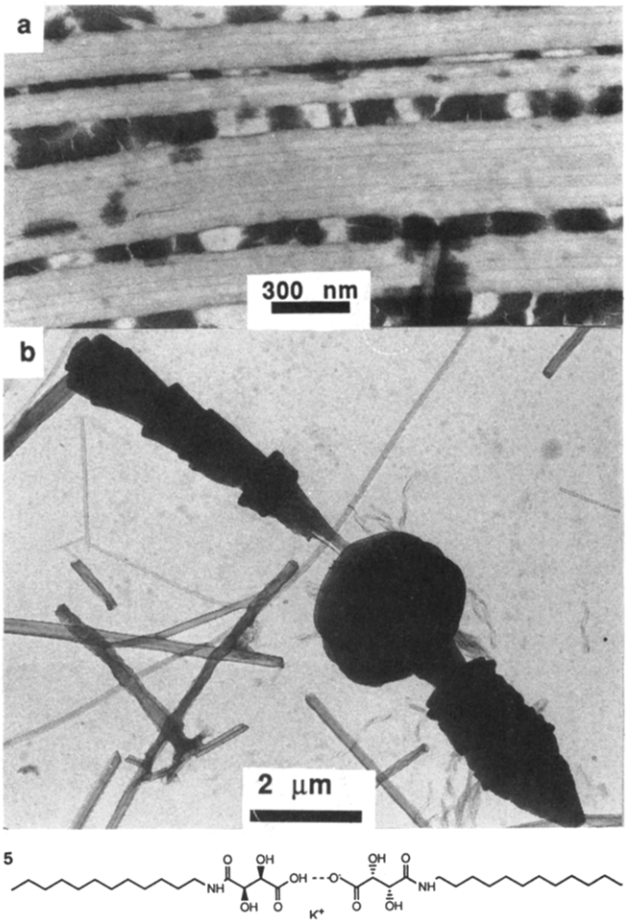

Figure 7. Tartaric acid amide **5** dissolves in water above pH = 7. At pH = 5, micellar fiber bundles (a) and micellar cloths (b) are formed.[24]

amide aggregates are probably singular, but have a high tendency to align parallel to form cylinders and cloths. Other micellar fibers have not been investigated in detail; they consist probably at least of double strands. Common to all these rod structures is a pronounced rigidity, which prevents the merging of fibers at crossing points and their flattening on the electron microscopic grid.

The observations on fluid and solid rod structures made of lipid bilayers in an aqueous environment can be summarized as follows:

Fluid rods are made by slow swelling processes of water-insoluble multilayer systems or by fusion of vesicles. They consist of multiple bilayers, their diameter is in the range of micrometers. They do not form bundles of parallel fibers but show many irregular foldings. Their appearance is changing from linear rods to complex mixtures of helices and finally mosaic structures. The repulsive forces between the head groups are stronger than the corresponding binding forces.

Solid rods are, on the other hand, made by fast precipitation reactions, e.g. cooperative formation of hydrogen bond chains at a given temperature or neutralization of carboxylate end groups. Their diameter is in general not larger than 12 nm; under appropriate conditions the ultimate thinness of ~4 nm of a molecular bilayer is reached. Solid fibers tend to align in bundles, because they are rigid. A multiplicity of four seems to be favored. The binding forces between the head groups in the single fibers are stronger than the repulsion forces.

The *lifetime* of fluid rods is in the order of hours in water. To the best of our knowledge it cannot be prolonged by any means. The semisolid rods made of cetyltrimethylammonium salicylate, on the other hand, practically live forever, and the solid rods made of *N*-octyl-D-gluconamide for more than 6 months if SDS is added.[20] Spherical micelles which are probably present in both systems presumably dissolve developing crystallites and thus protect the metastable fibers from irreversible crystallization.

A most surprising rod structure has been reported by Newkome,[25] namely the molecular monolayer assembly of the arborol **6**. The multitude of amide groups obviously binds the bolaamphiphiles so tightly together in an aqueous environment, that the hydrophobic effect can be negligibly small. This fiber is certainly only formed by binding head-group interactions, a contact between the oligomethylene chains is almost impossible (Figure 8).

III. Tubules and Ribbons

Lipid tubules constitute ultrathin capillary tubes and provide concave surfaces with the functionality of the head groups. If the walls of these capillaries are thin enough, the concave surface may be transported to the outer surface, when these tubules collapse in vacuo in

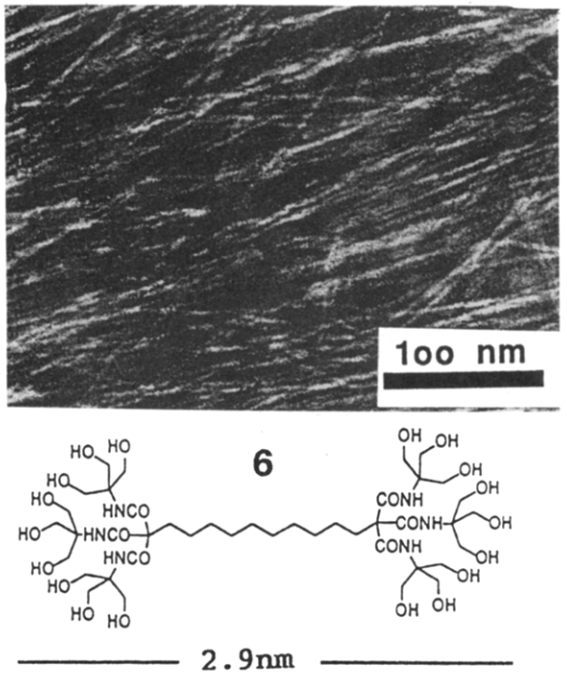

Figure 8. The first example of an electron micrograph of monolayered rods with a diameter that is identical to the length of the bolaamphiphilic arborol molecule (2.9 nm). Reprinted from ref 25. Copyright 1990 American Chemical Society (with kind permission of Prof. G. R. Newkome).

the same way as vesicles collapse, when the inside water is evaporated.[26] This surface will again contain the polar head groups in a concave orientation and can be considered as a model of enzyme clefts. Here lies the major interest in tubule structures. Bilayer ribbons and twisted ribbons are often found as precursors and/or side products of tubules. They are of no obvious use in bioorganic chemistry.

Soft ribbons and tubules with diameters of about 0.1–1 μm are found on the surface of plant epiticula[27a,b] (Figure 9). Similar tubes can be obtained if a typical wax, e.g. the long chain alcohol 10-eicosanol (**7**), is precipitated from chloroform solution.[28]

The same swelling process of water-insoluble amphiphiles, e.g. lecithin and synthetic analogues, that produce rods (Figure 3) may also lead to water-filled tubular vesicles (Figure 10). The surface of these closed tubular structures of light-microscopic dimensions is again of fluid character, the size and shape of the tubules are constantly changing.[29,30] Addition of hydrophobic dextran derivatives leads to strings of vesicles (see section 5).

Ultrathin molecular bilayer ribbons and rubules are in general formed from amphiphiles that are less soluble than those that form rods. A first example is *N*-octyl-D-galactonamide (**8**), a diastereomer of the rod-forming *N*-octyl-D-gluconamide (**3**) (see Figure 5). **8** is about 100 times less soluble than **3** and forms mixtures of straight and twisted ribbons upon cooling[9] (Figure 11a). The width of the ribbons (~50–100 nm) is about 10 times as large as the bilayer thickness. Very similar ribbons have been obtained from *N*-octyl-D-gluconamide in 1,2-xylene, where this diastereomer is much less soluble than in water. Helical ribbons of different widths and shapes were also obtained in organic solvents from 12-hydroxystearic acid (**9**), with a single chiral center in the hydrophobic chain. Width and shape of

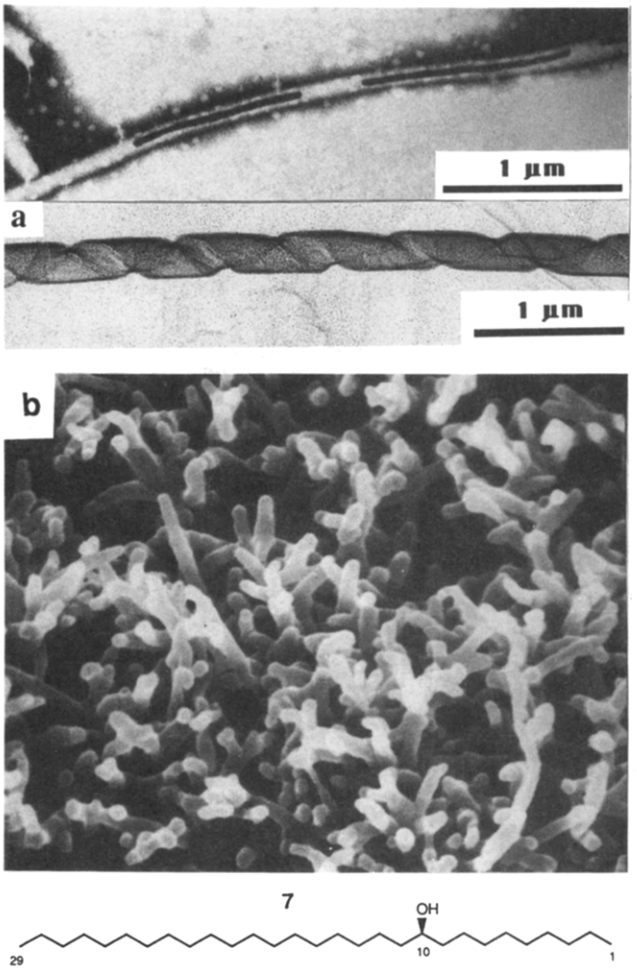

Figure 9. Electron micrographs of (a) two lipid tubules observed on the surface of barley leaves and (b) 10-eicosanol (**7**) (a chiral stereochemistry of the natural product is not known) tubules on needles of fir. Similar tubules are obtained by evaporation of chloroform solutions. From ref 27a,b (by kind permission of Prof. M. Riederer and Prof. Penny von Wettstein-Knowles).

the ribbons are here very much dependent on the metal counterions (different alkali ions) and solvents (hydrocarbons, alcohols). In the case of the free acid in nonanol it was also found that several thin helical rods intertwine to form broad helical ribbons.[17,18] Most twisted ribbons have, however, been produced from double chain amphiphiles with chiral amino acid, phosphatidyl, or nucleotide head groups. If 1,2-bis-(10,12-tricosadiynoyl)-sn-glycero-3-phosphocholine (**10**) was precipitated from alcohol solutions with water, then first twisted ribbons (80% methanol) were observed, which later closed to form tubules (see section 5, Figure 22).[31]

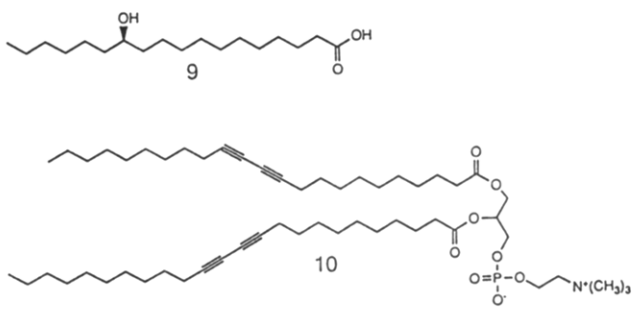

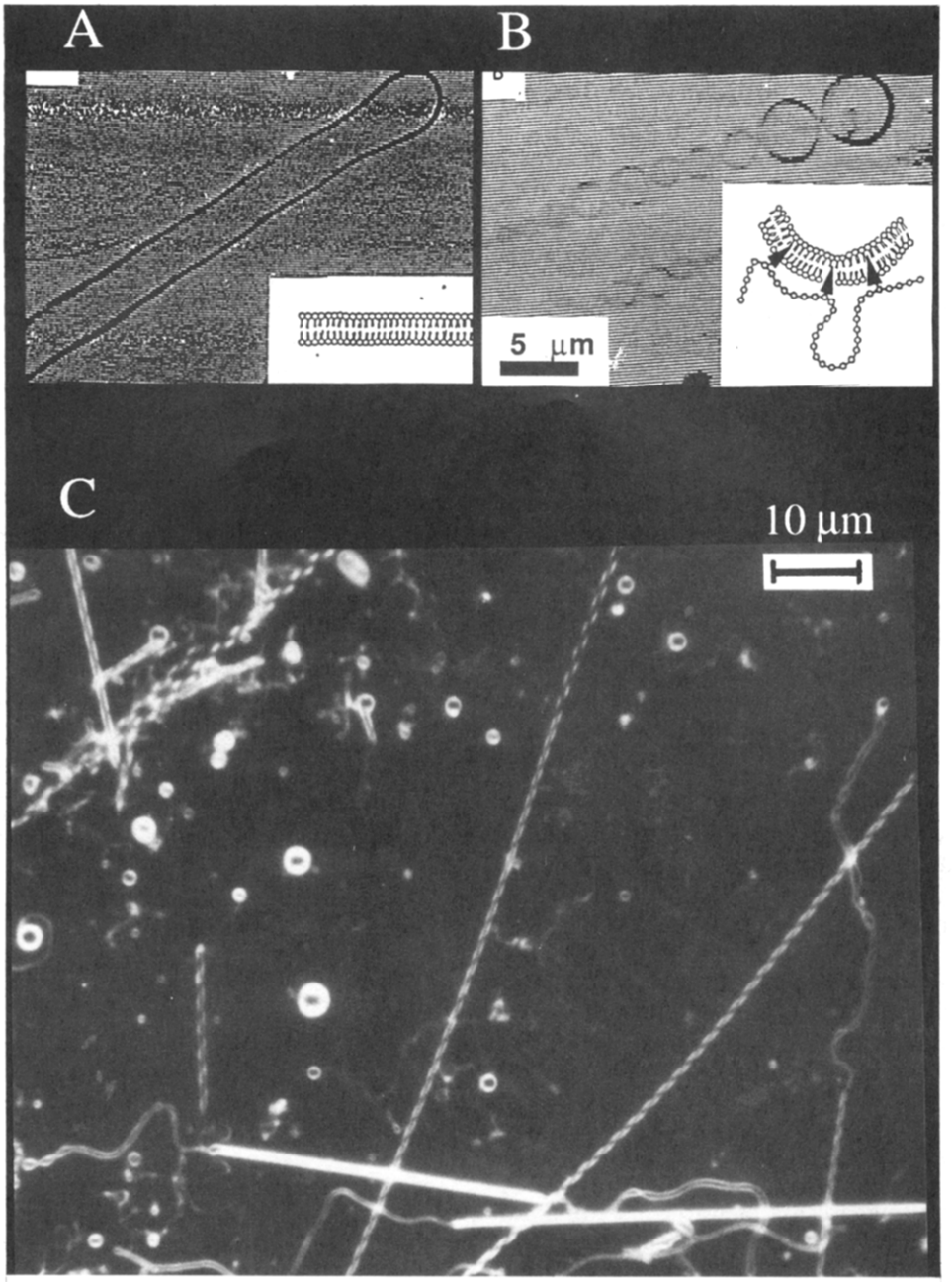

Figure 10. Part A shows a light micrograph of liquid multilayered tubular vesicles made of DMPC formed by swelling of crystallites in water. Part B show the splitting of the same tubules after the addition of dextran with a few hydrophobic side chains (see section 5)[29,30] (by kind permission of Prof. H. Ringsdorf). Part C shows Barkfield, light micrograph of solid helical ribbons, toroids, and tubes made of double chain glutamate **12** (see Figure 11)[37] (with kind permission of Prof. T. Kunitake).

In aqueous suspensions such ribbons were obtained from the double-chain nucleotide **11** from similar glutamate and aspartate derivatives, such as **12**[32,33] (Figure 11, parts b and c). In both cases the amphiphiles were first dispersed in vesicular form by ultrasonication and then left standing for several hours. The vesicles budded out to form first short rods with a diameter of ca. 11 nm and then characteristic long twisted ribbons with somewhat irregular pitches between 50 and 60 nm and a width of about 15–30 nm. The nucleotide ribbons grew to lengths of several micrometers and later filled up to form tubules (see section 5) within one week. Helical ribbons of amino acid amphiphiles not only grew in length but also in width.[34–38] They show the characteristics of short rods and the helical ribbons, and tubules are seen not only under the electron microscope, but also under the light microscope.[37] The helical pitches then grow to 3.2 μm, the ribbon width to 1–3 μm.[38]

The appearance of twisted ribbons is thus much less uniform than the appearance of rodlike helices. Both the widths and the pitches vary by several orders of magnitude. A major problem, which has not yet been addressed experimentally, is the organization of the edges. There is probably an area of micellar curvature which covers the hydrophobic edges, but this cannot be demonstrated by molecular spectroscopies as long as it is not possible to obtain pure ribbon preparations without vesicles, rods, and other impurities.

Toroids have been only observed occasionally. The most spectacular observation concerns the slow con-

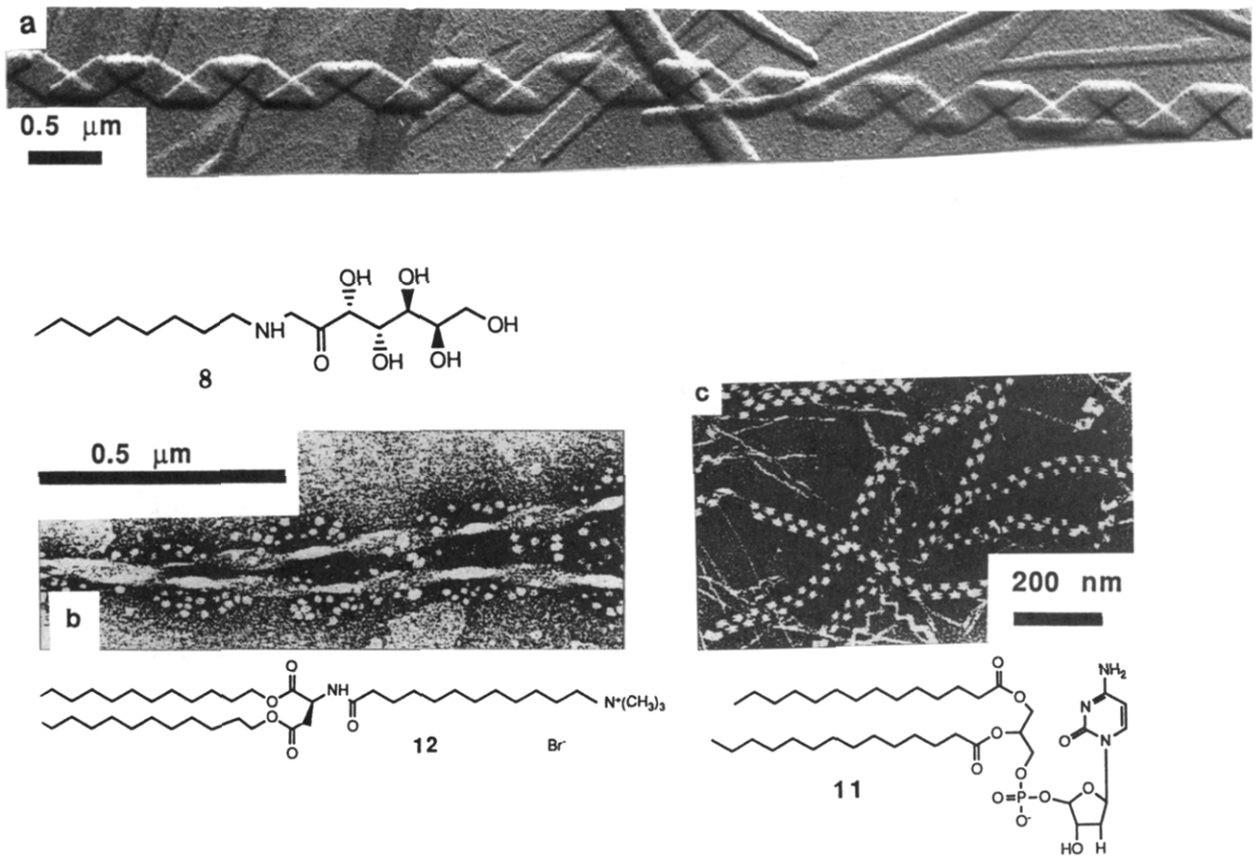

Figure 11. Electron micrographs of helical ribbons made of (a) *N*-octyl-D-galactonamide (**8**), (b) a double-chain glutamic ester with a tetraalkylammonium head group **12**[34] (by kind permission of Prof. T. Kunitake), and (c) a double-chain phospholipid with a nucleotide head group **11**[33] (by kind permission of Prof. H. Yanagawa). All three amphiphiles also form tubules.

version of vesicles made of 5′-phosphatidylcytidine **11** to circular helical strands with a diameter of 50–150 nm in presence of 0.2 M KCl.[32] At lower KCl concentration (0.01–0.05 M) linear helical strands were produced, at higher KCl concentrations (0.5–1.0 M) the vesicles remained intact. Only the phosphate anion (pH 8) showed this effect; in acidic solution the vesicles remained unchanged by KCl additions (Figure 12a). Toroids with diameters of several micrometers have been obtained from partly polymerized 1,2-di-10,12-tricosadiynoyl-*sn*-glycero-3-phosphocholine (**10**) (Figure 12b). Such toroidal vesicles occur occasionally and are as stable as other vesicles.[39] Quite often one finds rods which look like stacked disks.[21,40,40–42] The electron micrographs of these stacks often do not reveal, if the rod is hollow or not. In aged *N*-octyl-D-gluconamide (**3**) gels, however, the tube walls were identified as single spiraling fibers. Furthermore the toroids have a very regular thickness of a molecular tetralayer, arranged at an angle of 80° against the rod's axis[21] (Figure 12c).

The reversible fusion of vesicles instead of micelles leads to multilayered tubules. The first example was the formation of short cylinders by addition of ≥ 1 mM calcium chloride to phosphatidylserine **13** microvesicles. A white flocculate was formed which cleared after addition of EDTA (10 mM). Only the flocculate contained cylinders which converted to giant vesicles (diameter ≈ 1 μm) after removal of calcium ions with EDTA. The repulsion of the reintroduced negative charges not only unraveled the multilayer cylinders but also converted the primarily formed sheets to vesicles by fusion at the edges.[43]

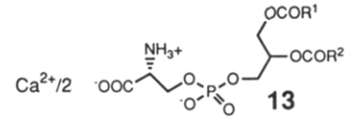

R^1, R^2 alkyl chains of fatty acids

Thinner (0.5 μm) and relatively longer (10–200 μm) tubules are obtained from amphiphiles, which contain diacetylenic units in the fatty acid chains, e.g. **10**. These tubules were formed either by precipitation from ethanolic solution with water without vesicle formation[31] or by slow cooling of aqueous vesicular solutions.[44] Tubule growth then occurred by continuous transfer of lipid bilayers from vesicles by a rolling-up process as shown by light microscopy. Tubule growth never started from isolated vesicles, but from contacting areas between liposomes and from already existing tubules.[44] It is unlikely, that the addition of monomers plays a significant role in tubule growth. The extremely low solubility of lecithin monomers in water ($\leq 10^{-10}$ M) practically rules this out. The growth mechanism and low solubility keep such tubules relatively short. Longer tubules are obtained if organic or micellar solutions of appropriate amphiphiles, e.g. *N*-octylmannonamide (**14**, Figure 13), are cooled down.[9] Here the formation of hydrogen bond bridged bilayer sheets should occur first, and they roll up to form long, cigar-type scrolls (see Figure 2). A similar mechanism occurs with helical

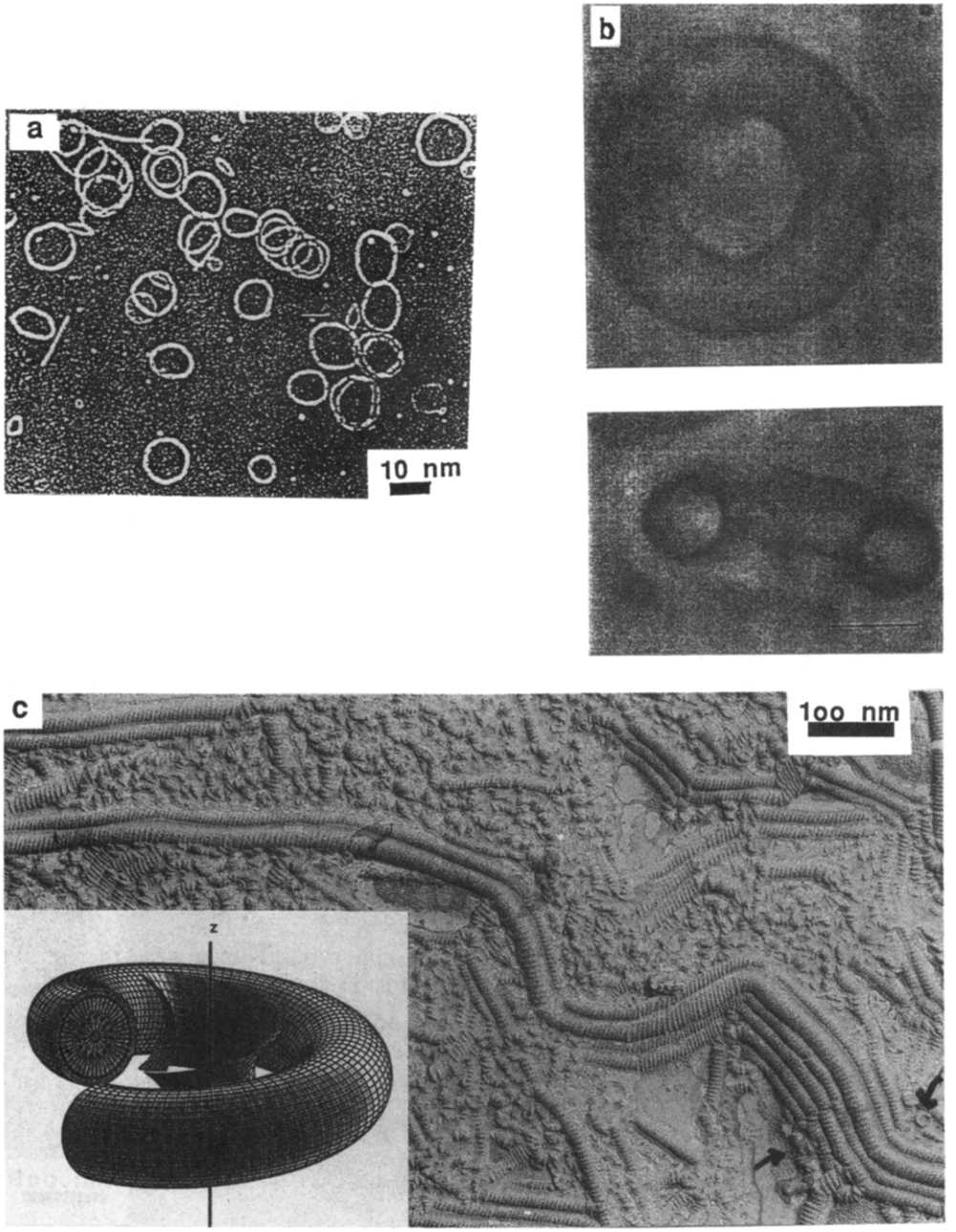

Figure 12. Micrographs of toroids (a) made by rearrangement of glyceronucleotide **11** vesicles by salt addition, (b) by swelling of polymerizable phospholipid **10**, and (c) by spontaneous rearrangement of rodlike helices made of **3** to tubular helices.[21]

ribbons as precursors. When the amphiphile is soluble enough, gaps in helical ribbons are filled in within days or weeks and tubules are formed.

The thinnest and longest tubules so far have been made from *N*-alkyl-D-gluconamides **15** with diacetylene groups in the single side chain. These compounds form helical ribbons. The gaps are usually filled up rapidly, and tubules with inner diameters of 8–12 nm are formed.[45] Similar tubular rods have been observed with the potassium salt of the tartaric amide **6**.[24] The hollow center of these assemblies can become as thin as 4 nm, the length to diameter ratio rises above 10^3. These tubules are quite rigid, showing almost no bending and form viscous solutions rather than gels.

Three types of lipid tubules may be distinguished, namely (i) gapless helices or twisted ribbons that wind around a hollow center, (ii) rolled-up bilayer sheets, and (iii) micellar rods in cubic or hexagonal assemblies. Only types i and ii have been clearly identified so far (e.g. Figure 13).

IV. Chiral Bilayer Effects

Most of the micellar rods, ribbons, and tubules discussed so far are made of chiral molecules. Drastic changes of shapes are often observed if the enantiomeric amphiphile is added to these molecular assemblies. A few examples will illustrate these important effects. The quadruple helix of *N*-octylgluconamide **3** (Figure 5) is right-handed with the D enantiomer and left-handed with L enantiomer. A racemate only forms platelets without any curvature.[8] 12-D-hydroxystearic acid (**9**) and its L enantiomer form twisted ribbons with mirror-image foldings. The racemate again only gives platelets.[46] The same effect is found with tartaric acid amides.[24]

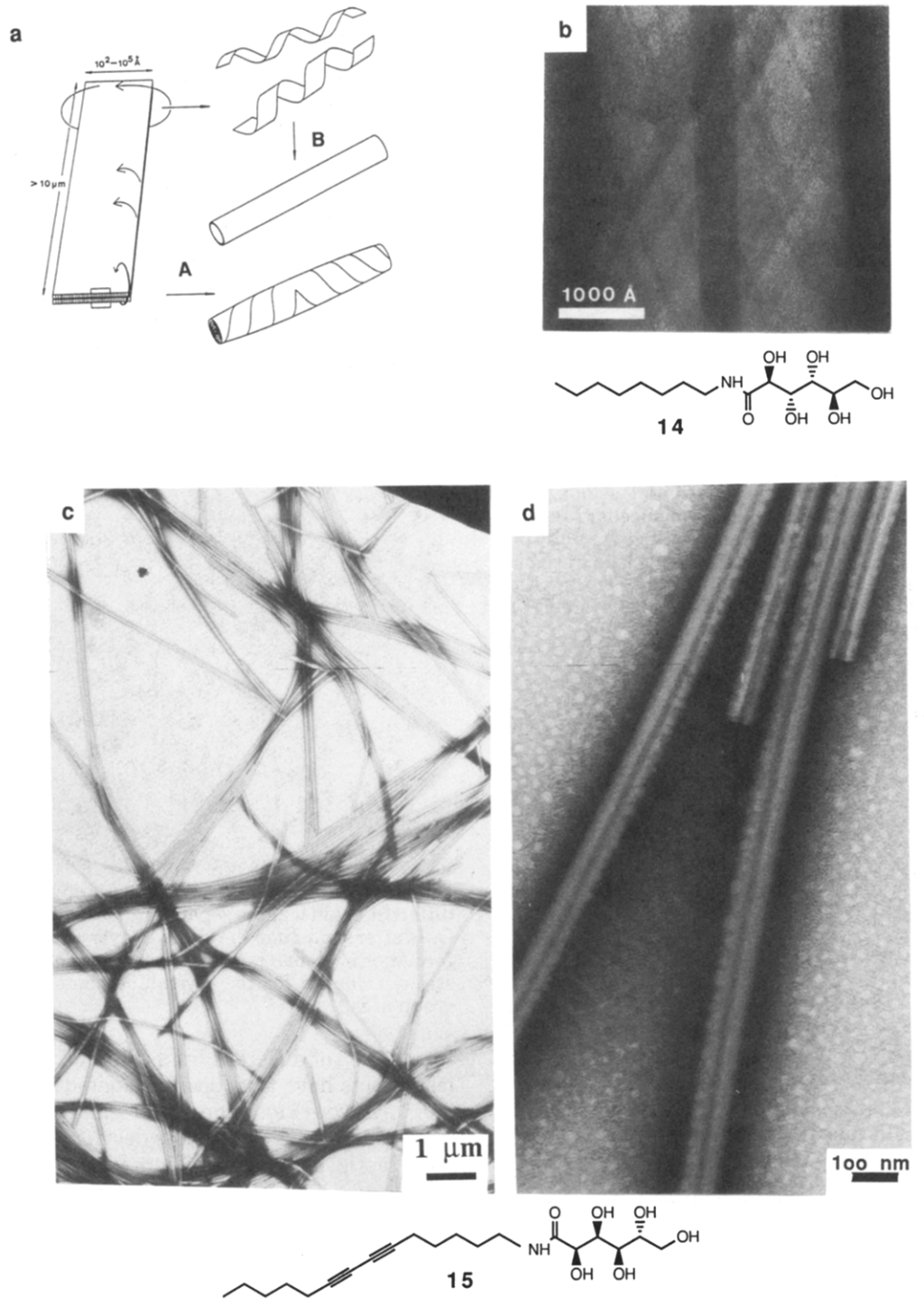

Figure 13. (a) Schematic representation of (A) scroll formation from planar bilayers and (B) tubule formation from helical ribbons. Electron micrographs of (b) a section of a mannonamide **14** scroll[9] and (c and d) self-organized tubular micelles made of the diacetylenic gluconamide **15**. The central hole has a diameter of about 12 nm.[45]

Racemic mixtures of galactonamides **8**, on the other hand, form elastic fibers without helical twists.[9]

The given examples indicate, that the effect of chirality on molecular assemblies seems to be directly related to curvature. Circular helical bilayers with high curvature and relatively small pitches are converted to platelets, if the enantiomer is added (*N*-alkylgluconamides, 12-hydroxystearic acid), whereas twisted ribbons are converted to straight ribbons or tubules (*N*-alkylgalactonamide **8**, glutamic acid amide **12**). In both cases the edge energy is considerably lowered in the racemates (Figure 14).

V. Mixed Systems

Lecithin and taurochenodesoxycholate (**16**) in a 3:1 mixture first produce micellar disks with an diameter of about 30 nm upon sonication.[42] These disks pack to irregular stacks (Figure 15). It is thought that the steroidal surfactant accumulates at the edges of the disks and reduces the energy of the edges. Only upon further sonication (3 hours!) the steroidal domains become evenly distributed within the lecithin bilayer and vesicles are formed. This experiment demonstrates clearly the unique property of bilayer disks made of

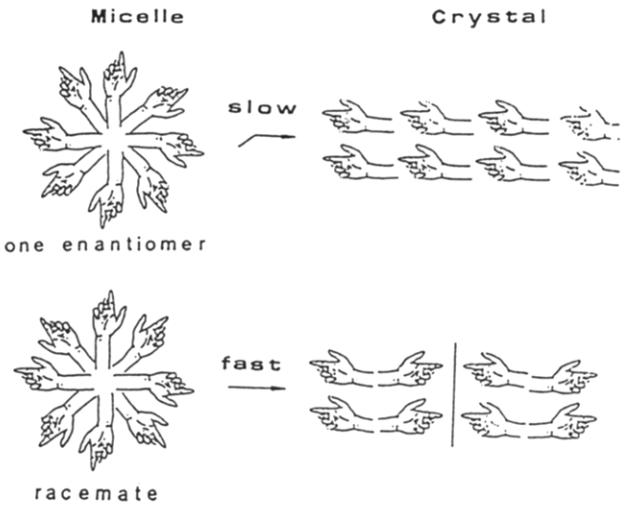

Figure 14. Illustration of the chiral bilayer effect.[8] Some chiral amphiphiles crystallize (a) in head-to-tail fashion. The rearrangement of the tail-to-tail bilayers in micellar fibers is slow. Therefore the micellar fibers are long-lived. (b) If the enantiomer of the chiral amphiphile is present, planar racemic crystals are rapidly formed. Uniform chirality is thus the presupposition here, to produce long-lived fiber systems of high surface energy.[8]

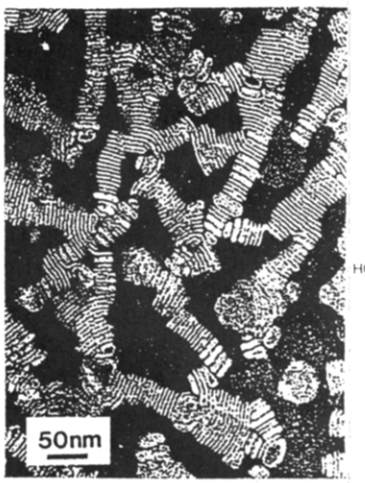

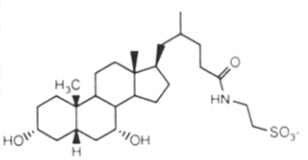

16

Figure 15. Rigid steroid amphiphiles, e.g. **16**, are thought to form domains in the more fluid lecithin 1 vesicles. These rigid domains transform the spheres to disks and form the edges of disk micelles, which then have a high tendency to form staples[43] (with kind permission of Prof. P. Fromherz).

only one amphiphile: there will always appear a region in which the hydrophobic chains will be exposed to the water surface. In the present case hydrophobic edge regions are covered with a domain of a bilayer-insoluble amphiphile.

If one adds water-soluble dextran containing some hydrophobic side chains to aqueous emulsions of tubular vesicles, the side chains will dissolve in the outer layer of the lipid bilayer of the tubules. The micellar polymer thus acts as a wedge only in the outer layer and induces curvature. As a result the tubule is split into a string of vesicles (see Figure 10). This is a polymer effect. Low molecular weight surfactants have the same effect only at 10^5-fold higher concentrations. It is the high local concentration of ancre groups, which makes the polymer so effective in a cooperative insertion into small segments of the membrane.[29,30]

In electron microscopy one can observe directly or after appropriate labeling the separation or "alloy formation" of different lipid assemblies. Stereochemical effects have thus been evaluated in the case of D- and L-glucon-, mannon-, and galactonamides being N-alkylated with octyl or dodecyl chains.[47]

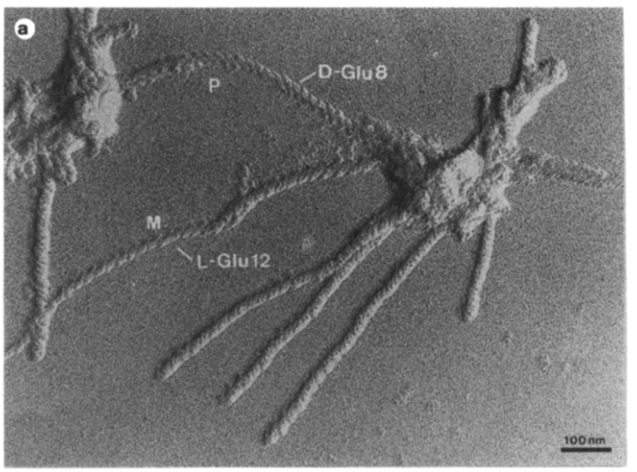

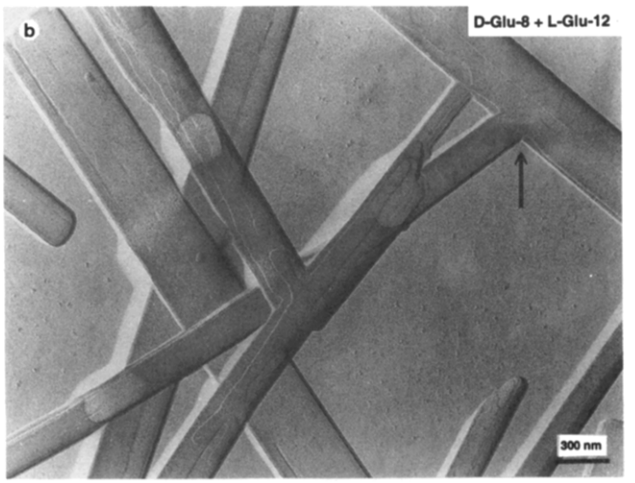

Figure 16. (a) Pseudo-enantiomers of amphiphiles with different chain lengths separate in form of P and M helices. Only after some time the chiral bilayer effect leads (b) to the formation of planar, racemic cocrystals. This finding provides strong evidence for the crystalline character of the headgroup area.[47]

A kinetic separation of fibers with enantiomeric head groups was, for example, found for *N*-octyl-D-gluconamide (D-Glu 8) and *N*-dodecyl-L-gluconamide (L-Glu 12). Within a few seconds right- and left-handed (= P, M) fibers separated (Figure 16a). Later planar crystals with pseudoracemic bilayers (Figure 16b) were formed.[47]

Diastereomeric glyconamides in 1:1 mixtures with the same hydrocarbon chains may also either completely mix or separate. Uniform tubules or separated multilayer scrolls and bilayer rods have been demonstrated for very similar pairs of diastereomers (Figure 17). These stereochemical differentiations could provide a unique methodology in the construction of molecular machinery in bulk media. Successful cocrystallization of reactive amphiphiles is a prerequisite.

The admixture of detergents, e.g. SDS, to lipids prolongs the lifetime of molecular assemblies with large specific surfaces. This is probably caused by the dissolution of crystallites, which would trigger irreversible destruction of the fibers, by the detergent. The quadruple helix of *N*-octyl-D-gluconamide (**3**, Figure 5) has been kept for 7 months at 60 °C and in presence

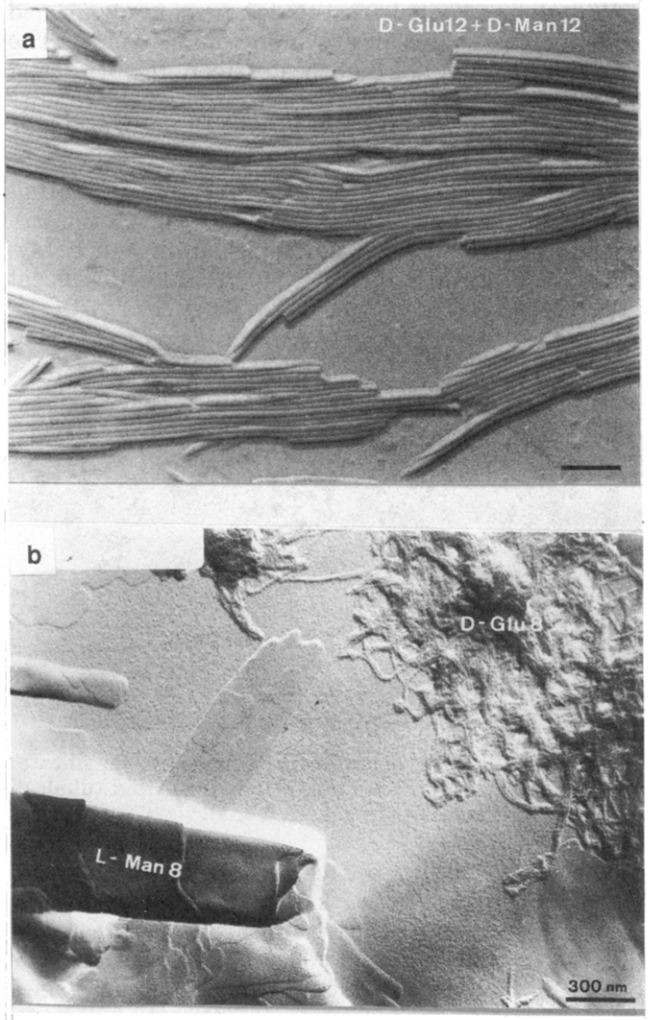

Figure 17. (a) D-Configurated, diastereomeric glucon- and mannonamides form uniform tubules ("alloys"), whereas (b) an analogous 1:1 mixture of D-glucon- and L-mannonamide separate quantitatively into scrolls and helical rods.[47]

of SDS. Under these conditions the individual fibers are constantly dissolved and rebuilt; the fibrous system as a whole, however, lives for a very long time. No change of the electron microscopic image was apparent (Figure 18).[20]

Useful molecular assemblies must be functional. Most important they should dissolve redox-active dyes. Bixin is a natural bolaamphiphilic carotene with ester and carboxylate end groups. It was derivatized with ethylene diamine and gluconic acid to yield the D-gluconamide **17**. Circular dichroism spectra of this compound dissolved in P and M fibers made of *N*-octyl-D- and L-gluconamides corresponded to mirror images (Figure 19).[48] The linear chromophore is thus fully integrated into the micellar fiber.

The same experiment with the protoporphyrin derivative **18**, on the other hand, gave complete separation. The porphyrin itself formed fibers,[49] which did not interact with the *N*-octyl-D-gluconamide fibers (Figure 20). These porphyrin fibers are relatively short twisted ribbons and form extremely long-lived (≥6 months), light-stable suspensions with almost no fluorescence. Similar fibers may be formed from zinc 5,15-dipyridyl-10,20-diphenylporphyrinate[50] and from protoporphyrin itself,[51] but have not been characterized by electron microscopy. There is, however, one report on porphyrin

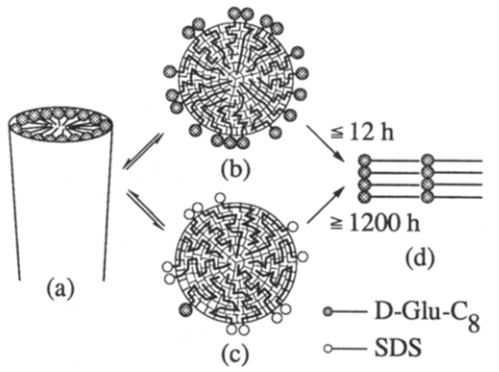

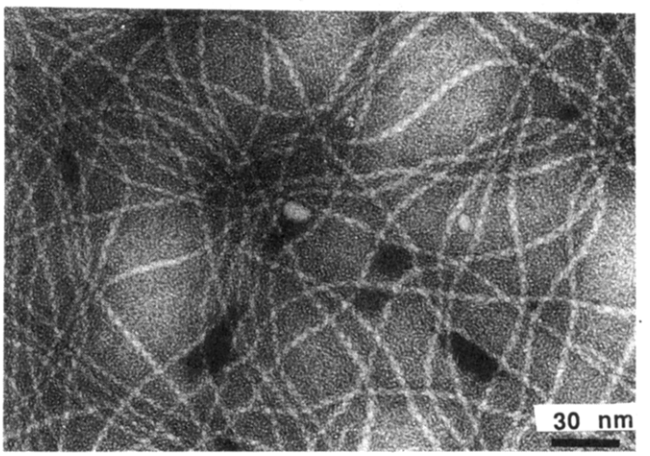

Figure 18. If one adds detergents, e.g. SDS, to the micellar fibers of *N*-octylgluconamide they become stable for months. Presumably the added micelles prevent the formation of crystals with head-to-tail orientation of the sheets (cf. Figure 5).[20]

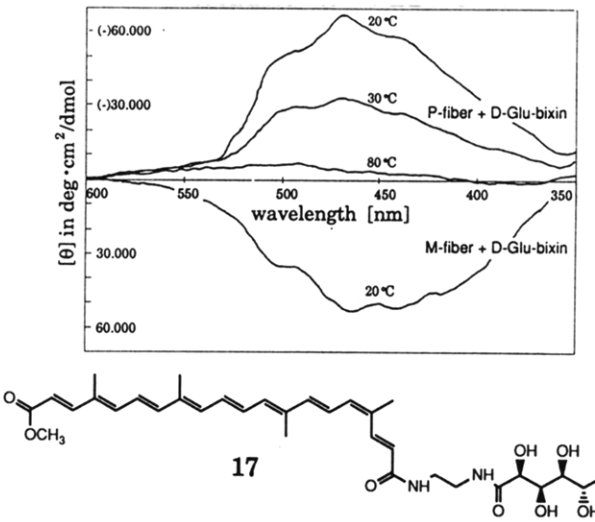

Figure 19. Other evidence for cocrystallization of glyconamide amphiphiles comes from the entrapment of carbotenoid gluconamide **16** in P and M fibers of *N*-dodecyl-D and -L-gluconamides. Mirror image circular dichroism is induced in both fibers.[48]

micellar ribbons made of 5-(4-*N*-hexadecylpyridiniumyl)-10,15,20-triphenylporphyrin bromide.[52] These ribbons are perhaps of bilayer thickness and about 50–100-nm wide.

It is also possible to coat lipid fibers with thin metal layers by "electroless plating". Here the lipid fiber spontaneously absorbs colloidal platinum or palladium particles from the bulk solution, which then act as nuclei

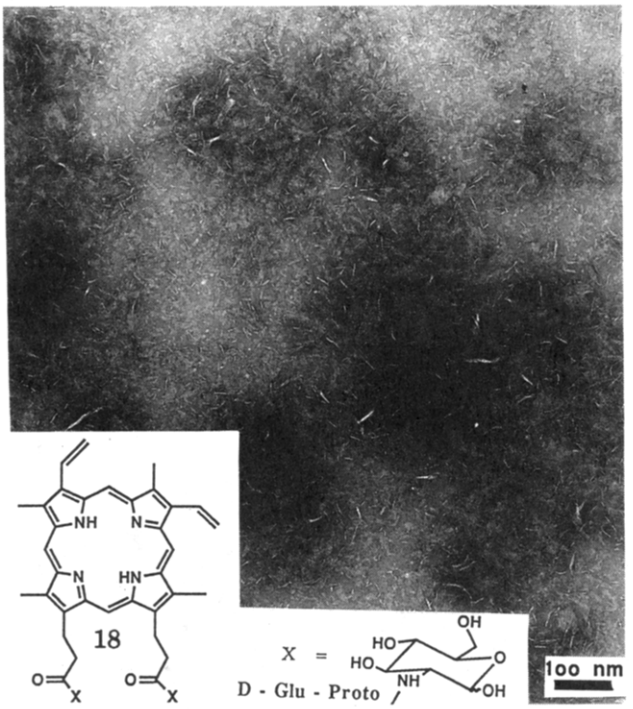

Figure 20. The protoporphyrin 2-aminoglycosamide 17 did not integrate into *N*-dodecyl-D-gluconamide. It rather formed separated fibers of its own.[43]

for the formation of closed sheets made of copper or nickel.[53] It is not yet known how thin and stable these metal coatings are, but light active and conducting lipid fibers of molecular dimensions are now in reach.

VI. Analogous Polymers

The supramolecular structures of lipid aggregates are determined by the hydrophobic effect, hydrogen bonds, charge interactions, and chirality of the head groups and side chains. The same interactions are most important in many amphiphilic polymers. We cannot, of course, review all of the relevant polymer structures, polymer mixtures and cocrystals here. A few general remarks and crossreferences are, however, thought to be a necessary complement.

Rod-shaped amphiphilic polymers may occur in aqueous dispersion in the liquid[54-56] or crystalline[57-58] state. Polymers with a fluid surface dissolve other polymers and dyes,[59] polymers with a crystalline arrangement cocrystallize.[58,59] Most important are the cocrystallization of inorganic phosphates with collagen[60] and the regioselective attachment and intercalation of dyes to nucleic acids.[58,61] In both types of biopolymers, proteins and nucleic acids, the partners in molecular complexes are either bound to the surface of a helical rod, or slip into clefts within or between helices.

The biopolymer–dye interaction may be so specific, that site-directed photolysis of the polymer chain can be achieved.[61] Such high degree of organization is not thinkable in lipid aggregates, and cleavage of assemblies will be difficult to detect. The biopolymers are thus better defined by the sequence of monomers than lipid aggregates ever will. Synthetic polymers, on the other hand, show to the best of our knowledge no well-defined supramolecular structures or selective interactions with other molecules. Ill-defined bundles of polymer fibers are in general observed under the electron microscope.[62]

Well-defined polymeric tubules are not only formed by biopolymers, but also by inorganic polymers. The best known example is the asbestos fiber. It is of interest here, because the concave hollow center of the tubules has a diameter of only 10 nm and thus corresponds exactly to the thin lipid tubules.

Asbestos fibers can be synthesized by "serpentinization" of olivine crystals, Mg_2SiO_4. Chrysotile is a bilayer silicate with a SiO_4 tetrahedron and a $Mg(OH,O)_6$ octahedron (brucite) layer. Since the repeat

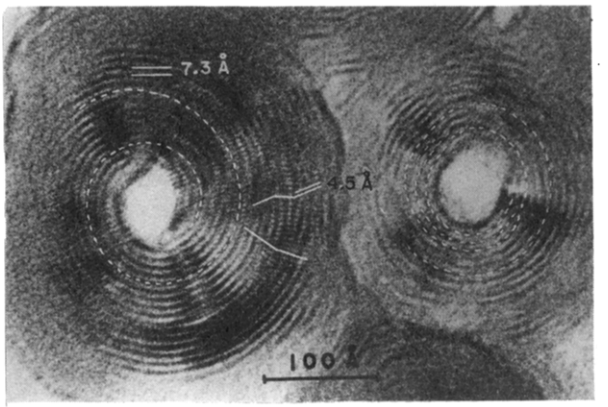

Figure 21. Inorganic asbestos fibers made bilayer silicates produce the same 8–12-nm hollow center as lipid tubules[63] (with kind permission of Prof. K. Yada).

distances of the brucite layer are slightly larger than those of the (Si_2O_5) network, the bilayer curls up. The silicate goes to the concave inner side, whereas $Mg(OH)_2$ is on the convex outside.[63] The curvature of the bilayer is limited by the distance of the lattice planes. The innermost layer has a typical diameter of about 10 nm, ten layers of 0.73 nm thickness follow, and an asbestos fibril then becomes 25–30-nm thick. The radial lattice fringes of 0.45 nm correspond to the silicate units.[63] The picture in Figure 21 corresponds perfectly to rolled-up lipid sheets. Radial growth stops, when the curvature becomes too low for serpentine bilayers. Length growth is unlimited and new material comes from the rearranging crystal (root growth).

Similar sheets with less curvature (inner radius $\approx$ 100 nm) can be made from carbon. Graphite whiskers are formed thermally from graphite crystals if the formation of a continuous layer of carbon is prevented. One either evaporates carbon in an electric discharge and condenses it on carbon surfaces,[65] or one uses a laser beam to heat the graphite.[66] Multilayered, sometimes bamboolike tubes were formed on graphitic materials. Outcrops of the basal planes of graphite at its surface are supposed to form the critical nuclei.

There are also several polymer analogues of aligned fibers in water. We name suspension of tobacco mosaic virus,[67] cellulose microcrystals,[68] and hemoglobin S.[69] Only the latter deserves to be discussed in connection with lipid assemblies. Hemoblobin S is a tetrameric protein with hydrophobic surface spots. It forms rigid rods which cluster in sickle cells to form preferrably square arrays.[69] Twisted ribbons are then formed, which are 50–90-nm wide,[70] and are followed by thicker and wider bundles of fibers (Figure 22), before large crystalling arrays of fibers precipitate.[71] It has also been shown, that addition of groups of monomers is

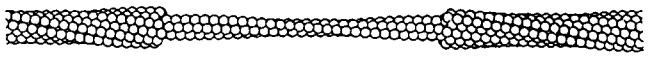

Figure 22. Sickle cell hemoglobin (=HbS) with a hydrophobic spot on the surface of the globular protein aggregates to form similar twisted ribbons and helical rods as observed in chiral micellar fibers. A typical low magnification electron micrograph of a twisted HbS ribbon is reproduced. The distance between crossover points is $4.4 \pm 0.2\,\mu m$[70]. Reprinted from reference 71. Copyright 1983 Benjamin/Cummings.

much favored over single additions and if more than one strand is elongated.[72]

Polymer and lipid sheets have also been used as matrices for the formation of specific inorganic crystals as models for biomineralization.[73,74] It seems obvious, that the lipid tubules and rods could serve similar purposes perhaps leading to ultrathin, elongated needles.

VII. Elasticity and Structure

So far, only molecular interactions have been made responsible for the formation of rods and tubules. Consideration of shape-dependent energies in terms of bending elasticities gives a more general picture. Let us first consider the theory of fluid aggregates which are not as complex as solid ones. Three elementary structures of fluid amphiphile assemblies may be distinguished: the spherical micelle, the extended cylindrical micelle, and the infinite bilayer. The simplest approach to predict which of the three occurs is based on geometry, using the cross section of the polar head and, in addition, the volume and maximal length of the hydrocarbon chain(s).[75] There is no shape energy in this theory so that the smallest shape compatible with the geometric constraints is preferred because entropy increases with the number of dispersed bodies.

Bending elasticity is a useful concept to deal with shape dependent energies. For both monolayers and bilayers in the fluid state the bending energy per unit area may be written in the form[76]

$$g = {}^1/_2K(c_1 + c_2)^2 - Kc_0(c_1 + c_2) + Kc_1c_2 \qquad (1)$$

Here c_1 and c_2 are the principal curvatures, c_0 is the so-called spontaneous curvature, K is the bending rigidity, and K the elastic modulus of Gaussian curvature. The last term is irrelevant for closed structures, i.e. vesicles, as the integral of Gaussian curvature, c_1c_2, over a closed surface is a topological invariant, depending only on the genus of the surface. On the other hand, a spontaneous curvature is characteristic of monolayers and common in the bilayers of closed vesicles as the exchange of molecules across them is usually very slow.

The bending elasticity of fluid bilayers permits the calculation of vesicle shapes as a function of area and closed volume which practically do not change with shape.[77-80] Other parameters are the spontaneous curvature, which can vary with shape, and the genus of the closed surface. Of particular interest in recent calculations was the problem of budding from vesicle membranes.[79-81] Such calculations can explain the formation of the string of beads displayed in Figure 10 and may bear on the budding of biological membranes. All the shapes calculated so far are axisymmetric or nearly so. Most of them have the topology of the sphere (genus 0), but toroidal shapes (genus 1) were also computed.[82,83] Toroidal vesicles have also been observed experimentally;[84] an example is shown in Figure 12.

Lipid membranes composed of chiral molecules, e.g. lecithins, have been used in most physical studies of vesicles. However, no effects of the chirality have been observed. This is, perhaps, not surprising as the molecules in fluid lipid bilayers are upright, i.e. of zero average tilt with respect to the layer normal (see below). As a rule, fluid bilayers do not stick to each other, even those that are electrically neutral. This appears to be a consequence of their strong thermal undulations or other out-of-plane fluctuations. Adhesion was induced in the case of mixed bilayers consisting of lecithin and cardiolipin by adding Ca^{2+} ions.[85] Myelin cylinders of pure lecithin also display mutual adhesion, forming double helices and other convoluted structures (see Figure 3), but not noticeably preferring one sense of winding over the other. The adhesion of the cylinders can be attributed to the suppression of membrane fluctuations in these compact multilayer systems.

We now turn to solid bilayers of amphiphiles with a crystalline surface. Such solid bilayers are usually made of short-chain amphiphiles such as *N*-octylgluconamide and similar molecules. They may be as flexible as fluid membranes because the hydrocarbon chains are short and probably not as well ordered as in polyethylene crystals. However, only cylindrical bending can be easily achieved since it does not require any area changes or shear of the layer. The occurrence of very regular tubules and helical ribbons of cylindrical bilayer curvature is therefore already clear evidence for the solid character of these bilayers. Another proof of crystallinity is the growth of long ribbons of constant width.

The gluconamide bilayers described above are probably anisotropic in their planes like other crystalline bilayers. Assuming cylindrical curvature $1/r$, r being the radius, we may write for their bending energy per unit area[86]

$$g = [{}^1/_2K_{ee}\cos^4\varphi + K_{ep}\cos^2\varphi\sin^2\varphi + {}^1/_2K_{pp}\sin^4\varphi](1/r^2) - K^*\cos\varphi\sin\varphi\,(1/r) \qquad (2)$$

where φ is the angle made by the direction of cylindrical curvature with one of the two optical axes of the two-dimensional crystal which are denoted by the subscripts e and p. The last term can be nonzero only if the symmetric bilayer is both anisotropic and composed of chiral molecules. It is the most interesting as it acts like the spontaneous curvature term in eq 1. In contrast to the latter, it changes sign as one varies φ, i.e. rotates the direction of curvature. Accordingly, the "chiral spontaneous curvature" can bend the bilayer either way. If the bending stiffness happens to be isotropic, eq 2 simplifies to

$$g = {}^1/_2K(1/r^2) - K^*\cos\varphi\sin\varphi\,(1/r) \qquad (3)$$

It is easy to see that this bending energy then has its minimum for $\varphi = \pm 45°$ and $r = 2K/K^*$. Equations 2 and 3 can account for the formation of bilayer tubules and helical ribbons such as those shown in Figure 5. Growing wider with time, at constant r, the helical

ribbons can close the gap between turns, thus becoming tubules. The gradient angle of the edges of the helical ribbon will be identical to φ if the strip grew along the p axis; it is exactly 45° only for an isotropic bending stiffness.

Incidentally, eq 2 with all its implications also holds for fluid membranes containing chiral molecules if the latter are collectively tilted with respect to the layer normal. Such layers exist in smectic C* liquid crystals but single membranes of this type still seem unknown.

There is an alternative mechanism to form helical ribbons which again requires chiral amphiphiles but no elastic anisotropy of the solid bilayer.[87] (Two-dimensional crystals of hexagonal symmetry are isotropic in this sense.) The origin of the second mechanism is a spontaneous torsion of the long edges of the ribbon, i.e. a tendency of the edge to rotate about itself. In the language of differential geometry torsion is defined as the rotation angle of the plane of curvature per unit length of line.

For a helix of radius r, the torsion is

$$\tau = 1/r \cos \varphi \sin \varphi \tag{4}$$

where φ is the gradient angle of the spiral. The total elastic energy of edge torsion and bilayer bending of a helical ribbon of isotropic bending stiffness may now be expressed by

$$G = {}^1/_2\lambda(\tau - \tau_0)^2(2A/w) + {}^1/_2K(A/r^2) \tag{5}$$

where A is the area, w the width, τ is the spontaneous torsion, and λ the elastic modulus of torsion (with dimension Jm). Minimizing eq 5, upon inserting eq 4, with respect to φ leads to $\varphi = 45°$ (or $-45°$, depending on the sign of τ_0). Minimizing G with respect to r after inserting this φ results in the equation

$$r = (Kw/\lambda + {}^1/_2)(1/\tau_0) \tag{6}$$

for the helix radius of minimal energy.

Note that according to eq 6 the helical radius increases linearly with the width of the ribbon, while eq 3, which governs the other mechanism of helix formation, predicts the helix radius to be independent of the width. Variations of the helical radius with ribbon width have been observed for most of the materials described above, but seem too small and irregular to be compatible with eq 6. However, there is a report on helical ribbons consisting of degradation products of phosphatidylcholine which obey this equation, the largest and smallest radii differing by a factor of 5.[88] When both mechanisms contribute, the equilibrium radius can be expressed by eq 6 with τ_0 being replaced by[86]

$$\tilde{\tau}_0 = \tau_0 + (w/2\lambda)K^* \tag{7}$$

The same two mechanisms that make ribbons helical can also produce twisted ribbons. Ideally, the principal curvatures of the bilayer should cancel each other in a twisted ribbon (i.e. $c_1 + c_2 = 0$) so that an isotropic bending rigidity has no effect on the energy of deformation. However, Gaussian curvature c_1c_2 does not vanish and the bilayer changes area or is sheared in twisted ribbons. A complete theory for twisted ribbons will have to take the associated energies into account.

Other solid structures found with chiral amphiphiles are fiber of various diameters which often form single or multiple helices. A bulgy arrangement of four helical rod micelles is formed by *N*-octyl-D-gluconamide (Figure 5). Smooth fibers twice as thick as the bilayer, mostly helical but sometimes straight, are also found.[21] They possibly constitute a first intermediate toward the planar head-to-tail arrangement which has been established for the monolayers in the final three-dimensional crystalline phase of this material. The same smooth fiber seems to form the hollow tubes consisting of a single spiral without gap between the turns (Figure 12c). The tubular structure is probably stabilized by self-adhesion through van der Waals attraction.

Helix formation of a fiber of isotropic circular cross section can be explained in terms of an elastic energy only if curvature terms of higher than the usual quadratic order are included. A sufficient form of the energy per unit length of fiber, g, was shown to be[89]

$$g = {}^1/_2k_2\kappa^2 + k_3\kappa^2\tau + {}^1/_4k_{22}\kappa^4 + {}^1/_2k_4[(\mathrm{d}\kappa/\mathrm{d}s)^2 + \kappa^2\tau^2] \tag{8}$$

where k_2, k_{22}, k_4, and k_3 are elastic moduli, the last occurring only in the case of chiral materials. Besides the curvature κ, the formula contains the torsion τ (defined as above) and, for completeness up to fourth order in κ and second order in τ, the derivative of κ with respect to length on the fiber. Putting $\partial g/\partial\tau = 0$, one finds the optimal torsion for any uniform curvature to be

$$\tau_0 = -k_3/k_4 \tag{9}$$

Inserting this in eq 8 yields

$$g = {}^1/_2(k_2 - k_3{}^2/k_4)\kappa^2 + {}^1/_4(k_{22}\kappa^4) \tag{10}$$

It is now easy to see that a negative g, i.e. the spontaneous formation of a helix, requires

$$k_3{}^2 > k_2k_4 \tag{11}$$

The fibers will remain straight if the inequality is not satisfied.

An example of generally straight fibers are those of chiral *N*-dodecyltartaric acid monoamides (see Figures 6 and 7). They are only one bilayer thick as are the strands of the quadruple helix of *N*-octyl-D-gluconamide (Figure 5). The latter evidently are helical like most of the twice as thick fibers of the same material. The bulginess of the quadruple helix suggests that helix formation is more important in lowering the free energy than the mutual adhesion of the strands.

The elastic theory for helical fibers presented here hinges on the assumption of circular isotropy. It does not matter whether the fiber is a cylindrical micelle or a stack of disks and whether the cross section is truly circular or hexagonal. On the surface of the solid micelle the polar heads of the molecules can be arranged in a lattice, in parallel circles, or in a single spiral. However, if the fiber consists of disks that are tilted with respect to its direction or if for other reasons there is no rotational symmetry, helix formation can be explained in terms of a theory which is quadratic in a set of three different rotations or curvatures.[90] There is also a hybrid theory of helix formation, developed to understand a biological phenomenon, that starts from an isotropic cylinder.[91] In this model the curvature of the

helical fiber induces the tilt which in turn lowers the energy of helix formation so much that it becomes negative.

VIII. Outlook

Semicrystalline micellar rods and tubules may constitute an ultrathin organic reaction medium in aqueous media. Dissolved dyes and redox or acid–base catalysts will always be within a nanometer or so of the bulk water. Adsorption and desorption of substrate to the large convex or concave surfaces could be very fast. In these respects the crystalline surfaces of the micellar fibers could have similar effects as those of nucleic acids and other biopolymers. Micellar fibers can, however, be easily prepared in kilogram quantities by self-assembly of simple monomers, whereas pure biopolymer fibers (nucleic acids, collagen, etc.) are expensive and of limited use for the integration of reactive compounds. Furthermore in contrast to synthetic amphiphilic polymers the assembly fibers have a much lower tendency to form ill-defined agglomerates. The molecular assemblies can also be rejuvenated by a simple heating–cooling cycle after damage by the reactive system. It is also thought, that the semicrystalline assemblies offer some advantages over vesicular systems with liquid surfaces. It should be much easier to immobilize catalysts and substrates within the more "protein-like" fiber assemblies than in "fluid, membrane-like" vesicles. Charge-separation processes, which do not work in vesicles, may be possible in well-defined cocrystals of micellar fibers and amphiphilic porphyrins. The concave surface on the surface of collapsed or within intact tubules may provide means to concentrate substrates from the bulk water.

So far only the preparation, physical properties conservation, and structures of micellar fibers have been investigated. We hope, that the present review can serve as a useful starting point for investigations of organized reaction systems.

Acknowledgments. This work was supported by the Deutsche Forschungsgemeinschaft (Sonderforschungsbereich 312, Vectorial Membrane Processes) and the Fonds des Chemischen Industrie.

References

(1) Fendler, J. H. *Membrane Mimetic Chemistry*; Wiley: New York, 1982.
(2) Israelachvili, J. N. Intermolecular and Surface Forces; Academic Press: New York, 1985.
(3) Dill, K. A.; Flory, P. J. *Proc. Natl. Acad. Sci. U.S.A.* **1980**, *77*, 3115–3119.
(4) Fromherz, P. *Chem. Phys. Lett.* **1981**, *77*, 460–466.
(5) Menger, F. M. *Acc. Chem. Res.* **1979**, *12*, 111–117.
(6) Israelachvili, J. N.; Marcelja, S.; Horn, R. G. *Quant. Rev. Biophys.* **1980**, *13*, 121–200.
(7) Cevc, G.; Marsh, D. *Phospholipid Bilayers*; Wiley: New York, 1987; p 49ff.
(8) Fuhrhop, J.-H.; Schnieder, P.; Rosenberg, J.; Boekema, E. *J. Am. Chem. Soc.* **1987**, *109*, 3387–3390.
(9) Fuhrhop, J.-H.; Schnieder, P.; Boekema, E.; Helfrich, W. *J. Am. Chem. Soc.* **1988**, *110*, 2861–2867.
(10) Sakurai, I.; Karvamura, T.; Dakurai, A.; Kegami, A.; Setoi, T. *Mol. Cryst. Liq. Cryst.* **1985**, *130*, 203–222.
(11) Bangham, A. D.; Horne, R. W. *J. Mol. Biol.* **1964**, *8*, 660–668.
(12) Bangham, A. D.; Hill, M. W.; Miller, N. G. A. In *Methods in Membrane Biology*; Korn, E. D., Ed.; Plenum Press: New York, 1974; pp 1–68.
(13) Lorenzen, S.; Servuss, R.-M.; Helfrich, W. *Biophys. J.* **1986**, *50*, 565–572.
(14) Saikaigudin, Y.; Shikata, T.; Urakami, H.; Tamura, A.; Hirata, H. *J. Electron Micros.* **1987**, *36*, 168.
(15) Hoffmann, H.; Ebert, G. *Angew. Chem.* **1988**, *100*, 933–944.
(16) Manohar, C.; Rav, U. R. K.; Valaulikar, B. S.; Iyer, R. M. *J. Chem. Soc., Chem. Commun.* **1986**, 379–381.
(17) Clausen, T. M.; Vinson, P. K.; Davis, H. T.; Talmon, J.; Miller, W. G. *J. Phys. Chem.* **1992**, *96*, 474–484.
(18) (a) Tachibana, T.; Kitazawa, S.; Takeno, H. *Bull. Soc. Chem. Soc. Jpn.* **1970**, *43*, 2418–2421. (b) Tachibana, T.; Yoshizumi, T.; Hori, K. *Bull. Chem. Soc. Jpn.* **1979**, *52*, 34–41.
(19) Pfannemüller, B.; Welte, W. *Chem. Phys. Lipids* **1985**, *37*, 227–240.
(20) Fuhrhop, J.-H.; Svenson, S.; Boettcher, C.; Rössler, E.; Vieth, H.-M. *J. Am. Chem. Soc.* **1990**, *112*, 4307–4312.
(21) Köning, J.; Boettcher, C.; Winkler, H.; Zeitler, E.; Talmon, Y.; Fuhrhop, J.-H. *J. Am. Chem. Soc.* **1993**, *115*, 693–700.
(22) Andersson, S.; Hyde, S. T.; Larsson, K.; Lidin, S. *Chem. Rev.* **1988**, *88*, 221–242.
(23) Bach, R.; Fuhrhop, J.-H. Unpublished results.
(24) Fuhrhop, J.-H.; Demoulin, C.; Rosenberg, J.; Boettcher, C. *J. Am. Chem. Soc.* **1990**, *112*, 2827–2829.
(25) Newkome, G. R.; Barker, G. R.; Arai, S.; Saunders, M. J.; Russo, P. S.; Theriot, K. J.; Moorefield, C. N.; Rogers, L. E.; Miller, J. E.; Lieux, T. R.; Murray, M. R.; Phillips, B.; Pascal, L. *J. Am. Chem. Soc.* **1990**, *112*, 8458–8465.
(26) Fuhrhop, J.-H.; David, H. H.; Mathieu, J.; Liman, U.; Winter, H.-J.; Boekema, E. *J. Am. Chem. Soc.* **1986**, *108*, 1785–1791.
(27) (a) Lister, G. R.; Thair, B. W. *Can. J. Bot.* **1981**, *59*, 640–648. (b) Wettstein-Knowles, P. V. *J. Ultrastruct. Res.* **1974**, *46*, 483–496.
(28) Hahn, A. Ph.D. Dissertation, Freie Universität, Berlin, 1992.
(29) Ringsdorf, H.; Schlarb, B.; Venomer, J. *Angew. Chem.* **1988**, *100*, 117–162.
(30) Kuchinka, E. Diplomarbeit, Universität Mainz, 1986.
(31) Georger, J. H.; Singh, A.; Price, R. R.; Schnur, J. M.; Yager, P.; Schoen, P. E. *J. Am. Chem. Soc.* **1987**, *109*, 6169–6175.
(32) Yanagawa, H.; Ogawa, Y.; Furuta, H.; Tsuno, K. *Chem. Lett.* **1988**, 269–272.
(33) Yanagawa, H.; Ogawa, Y.; Furuta, H.; Tsuno, K. *J. Am. Chem. Soc.* **1988**, *111*, 4567–4570.
(34) Nakashima, N.; Asukuma, S.; Kim, J.-M.; Kunitake, T. *Chem. Lett.* **1984**, 1709–1712.
(35) Yamada, K.; Ihara, H.; Ide, T.; Tukumoto, T.; Hirayama, C. *Chem. Lett.* **1989**, 1713–1716.
(36) Yamada, N.; Sasaki, T.; Muata, H.; Kunitake, T. *Chem. Lett.* **1989**, 205–208.
(37) Nakashima, N.; Asakuma, S.; Kunitake, T. *J. Am. Chem. Soc.* **1985**, *107*, 509–510.
(38) Kunitake, T.; Yamada, N. *J. Chem. Soc., Chem. Commun.* **1986**, 655–656.
(39) Mutz, M.; Bensimon, D. *Phys. Rev. A* **1991**, *43*, 4525–4527.
(40) Kunitake, T.; Okahata, Y.; Shimomura, M.; Yasunami, S.; Takarabe, K. *J. Am. Chem. Soc.* **1981**, *103*, 5401–5413.
(41) Inoue, K.; Suzuki, K.; Nojima, S. *J. Biochem.* **1977**, *81*, 1097–1106.
(42) Fromherz, P.; Röcker, C.; Ruppel, D. *Faraday Disc. Chem. Soc.* **1986**, 39–48.
(43) Papahadjopoulos, D.; Vail, W. J.; Jacobson, K.; Poste, G. *Biochim. Biophys. Acta* **1975**, *394*, 483–491.
(44) Yager, P.; Price, R. R.; Schnur, J. M.; Schoen, P. E.; Snigh, A.; Rhodes, R. G. *Chem. Phys. Lipids* **1988**, *46*, 171–179.
(45) Fuhrhop, J.-H.; Blumtritt, P.; Lehmann, C.; Luger, P. *J. Am. Chem. Soc.* **1991**, *113*, 7437–7439.
(46) Tachibana, T.; Yoshizumi, T.; Hori, K. *Bull. Chem. Soc. Jpn.* **1979**, *52*, 34–41.
(47) Fuhrhop, J.-H.; Boettcher, C. *J. Am. Chem. Soc.* **1990**, *112*, 1768–1776.
(48) Fuhrhop, J.-H.; Krull, M.; Schulz, A.; Möbius, D. *Langmuir* **1990**, *6*, 497–505.
(49) Fuhrhop, J.-H.; Demoulin, C.; Boettcher, C.; Köning, J.; Siggel, U. *J. Am. Chem. Soc.* **1992**, *114*, 4159–4165.
(50) Fleischer, E. B.; Shachter, A. M. *Inorg. Chem.* **1991**, *30*, 3763–3769.
(51) Inamura, I.; Uchida, K. *Bull. Chem. Soc. Jpn.* **1991**, *64*, 2005–2007.
(52) Guilara, R.; Senglet, N.; Liu, Y. H.; Sazon, D.; Findsen, E.; Faure, D.; Des Courieres, T.; Kadish, K. U. *Inorg. Chem.* **1991**, *30*, 1898–1905.
(53) Schnur, J. M.; Price, R.; Schoen, P.; Yager, P.; Calvert, J. M.; George, J.; Singh, A. *Thin Solid Films* **1987**, *152*, 181–206.
(54) Platé, N.; Shivaev, V. *Comb-Shaped Polymers and Liquid Crystals*; Plenum: New York, 1988.
(55) McArdle, C. B., Ed. *Side Chain Liquid Crystal Polymers*; Blackie: Glasgow, 1989.
(56) Weiss, R. A., Ober, C. K., Eds. *Liquid Crystalline Polymers*, American Chemical Society Symposium Series 435; American Chemical Society: Washington, DC, 1990.
(57) Squire, J. M., Vibert, P. J., Eds. *Fibrous Protein Structure*; Academic Press: London, 1987.
(58) Saenger, W. *Principles of Nucleic Acid Structure*; Springer: Berlin, 1983.
(59) Glass, J. E., Ed. *Polymers in Aqueous Media* American Chemical Society Advances in Chemistry Series 223; American Chemical Society: Washington, DC, 1989.

(60) Loewenstam, H. A.; Weiner, S. *On Biomineralization*; Oxford University Press: New York, 1989; pp 36ff.
(61) Mack, D. P.; Dervan, P. B. *J. Am. Chem. Soc.* **1990**, *112*, 4604–4606 and references cited therein.
(62) Fuhrhop, J.-H.; Spiroski, D.; Schnieder, P. *React. Polym.* **1991**, *15*, 215–220.
(63) Yada, K.; Iishi, K. *Amer. Mineral.* **1977**, *62*, 958–965.
(64) Yada, K. *Acta Crystallogr.* **1967**, *23*, 704–707.
(65) Bacon, R. *J. Appl. Phys.* **1960**, *31*, 283–290.
(66) Fedoseer, D. V.; Deryagin, B. V.; Varshawskaya, I. B.; Lavrent'ov, A. V. *Pokl. Phys. Chem.* **1975**, *221*, 229–231.
(67) Parsegian, A.; Brenner, S. L. *Nature* **1976**, *259*, 632–635.
(68) Marchessault, R. H.; Morehead, F. F.; Walters, N. U. *Nature* **1959**, *184*, 632–633.
(69) Crepeau, R. H.; Dykes, G.; Garrell, R.; Edelstein, S. J. *Nature* **1978**, *274*, 616–617.
(70) Wellems, T. E.; Josephs, R. *J. Mol. Biol.* **1980**, *137*, 443–450.
(71) Dickerson, R. E.; Geis, I. *Hemoglobin*; Benjamin/Cummings: Menlo Park, CA, 1983.
(72) Briehl, R. W.; Mann, S. E.; Josephs, R. *J. Mol. Biol.* **1990**, *211*, 693–698.
(73) Mann, S. In *Biomineralization*; Mann, S., Webb, J., Williams, R. J. P., Eds.; VCH: Weinheim, 1989; pp 35–62.
(74) Addadi, L.; Weiner, S. In *Biomineralization*; Mann, S., Webb, J., Williams, R. J. P., Eds.; VCH: Weinheim, 1989; pp 133–156.
(75) Israelachvili, J. N.; Mitchell, D. J.; Ninham, B. W. *J. Chem. Soc., Faraday Trans. 2* **1976**, *72*, 1525.
(76) See, for example: Helfrich, W. In *Les Houches, Session XLVIII, 1988 – Liquids at Interfaces*; Charvolin, J., et al., Eds.; Elsevier: Amsterdam, 1990.
(77) Deuling, H. J.; Helfrich, W. *J. Phys. Fr.* **1976**, *37*, 1335.
(78) Sevetina, S.; Zeks, B. *Eur. Biophys. J.* **1989**, *17*, 101.
(79) Seifert, U.; Berndl, K.; Lipowsky, R. *Phys. Rev.* **1991**, *A44*, 1182.
(80) Miaou, L.; Fourcade, B.; Rao, M.; Wortis, M.; Zia, R. K. P. *Phys. Rev.* **1991**, *A43*, 6843.
(81) Wiese, W.; Harbich, W.; Helfrich, W. *J. Phys.: Condens. Matter* **1992**, *4*, 1647.
(82) On-Yang, Z.-C. *Phys. Rev. A* **1990**, *41*, 4517.
(83) Seifert, U. *Phys. Rev. Lett.* **1991**, *66*, 2404.
(84) Fourcade, B.; Mutz, M.; Bensimon, D. *Phys. Rev. Lett.* **1992**, *68*, 2551.
(85) Lin, K.-C.; Weis, R. M.; McConnell, H. M. *Nature* **1982**, *29b*, 164.
(86) Helfrich, W.; Prost, J. *Phys. Rev.* **1988**, *A38*, 3065.
(87) Helfrich, W. *J. Chem. Phys.* **1986**, *85*, 1085.
(88) Servuss, R. M. *Chem. Phys. Lipids* **1988**, *46*, 37.
(89) Helfrich, W. *Langmuir* **1991**, *7*, 567.
(90) Helfrich, W. Unpublished.
(91) Pomeau, Y.; Lega, J. *C.R. Acad. Sci., Ser. 2.* **1990**, *311*, 1135.
(92) Fuhrhop, J.-H.; Mathieu, J. *Angew. Chem.* **1984**, *96*, 124–137; *Angew. Chem., Int. Ed. Engl.* **1984**, *23*, 100–113.